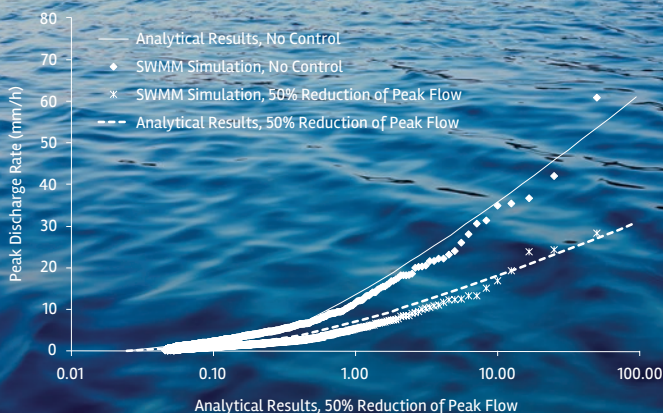




Statistical Analysis of Hydrologic Variables

Methods and Applications



Edited by

Ramesh S. V. Teegavarapu, Ph.D., P.E.

Jose D. Salas, Ph.D.

Jery R. Stedinger, Ph.D.



ENVIRONMENTAL &
WATER RESOURCES
INSTITUTE

Statistical Analysis of Hydrologic Variables

Methods and Applications

Edited by
Ramesh S.V. Teegavarapu
Jose D. Salas
Jery R. Stedinger

Prepared by the Task Committee on
Statistical Applications in Hydrology of the
Surface Water Hydrology Technical Committee of the
Environmental and Water Resources Institute.



Published by the American Society of Civil Engineers



CHAPTER 12

Hydrologic Record Events

Richard M. Vogel
Attilio Castellarin
N. C. Matalas
John F. England, Jr.
Antigoni Zafarakou

GLOSSARY

AM: Annual maximum series, which is the series of the largest value observed in each year; this series is often used in computations of flood frequency

Bivariate (multivariate) distribution: The joint distribution for two (n) random variables X_1 and X_2 (X_1, \dots, X_n) defined on the same probability space, which describes the probability of events defined in terms of both X_1 and X_2 (defined in terms of X_1, \dots, X_n)

Bivariate (multivariate) record (after Nagaraja et al. 2003): Let $\mathbf{X} = (X_1, X_2)$ [$\mathbf{X} = (X_1, \dots, X_n)$] be a bivariate (multivariate) random variable with an absolutely continuous cumulative distribution function or cdf, F and probability density function or pdf, f . Let F_j and f_j be the marginal cdf and pdf of X_j , $j = 1, 2$ ($j = 1, \dots, n$). Also let $\mathbf{X}(i) = [X_1(i), X_2(i)]$ [$\mathbf{X}(i) = [X_1(i), \dots, X_n(i)]$], with $1 \leq i \leq m$, denote a random sample of size m from F

DEFINITION 1: a bivariate (multivariate) record of *first kind* is said to occur at time k if both of $X_1(k)$ and $X_2(k)$ [all $X_1(k), \dots, X_n(k)$] exceed—or are smaller than— $X_1(i)$ and $X_2(i)$ [$X_1(k), \dots, X_n(k)$], with $i < k$

DEFINITION 2: a bivariate (multivariate) record of *second kind* is said to occur at time k if at least $X_j(k)$, with $j = 1, 2$ ($j = 1, \dots, n$) exceeds—or is smaller than—all preceding $X_j(i)$, with $i < k$

EEPE: Expected exceedance probability of an envelope; EEPE is the most appropriate summary measure if one's concern is with making a probabilistic statement regarding the single envelope based on historical observations

EPEE: Exceedance probability of the expected envelope; EPEE is the most appropriate summary measure if one's concern is with making a probabilistic statement regarding the envelope expected to occur for a group of sites of given characteristics (i.e., number of sites, record lengths, cross-correlation, etc.)

Exceedance probability: The likelihood or probability that a random variable will be exceeded

EXP: Exponential probability distribution

GEV: Generalized extreme value probability distribution

GPA: Generalized Pareto probability distribution

GUM: Gumbel probability distribution

HU: Hydrologic unit

Lower record: Smallest observed value of a random variable during a particular time period

Monte Carlo experiment: An experiment in which a series of random variables are generated and that series is then used to compute a particular statistic; by repeating the experiment over and over, one may generate a large sample of the particular statistic of interest whose behavior can then be explored

Parametric properties: Properties pertaining to a random variable when that random variable is assumed to follow a particular probability distribution

Plotting position: An empirical estimate of the nonexceedance probability associated with an observation of a random sample from a (possibly unknown) probability distribution

POT: Peaks over threshold, which denotes the series that results from removing all values of the original series below some threshold value

Quantile: Value of a random variable that is exceeded by some probability p , often denoted as x_p , where x is the random variable and p is the exceedance probability

Record: Largest or smallest observed value of a random variable during a particular time period

Record of the first kind: See Section 12.2.4

Record of the second kind: See Section 12.2.4

Record of the third kind: See Section 12.2.4

Record of the fourth kind. See Section 12.2.4

Recurrence interval. Length of time between two events such as the length of time between two floods

T: Average return period or time or recurrence interval between the occurrence of two events, or in the context of floods, the average time one must wait until the occurrence of the next flood event

Upper record: Largest observed value of a random variable during a particular time period

12.0 GENERAL

A record event is defined as an event whose magnitude exceeds, or is exceeded by, all previous events. One thing is certain: a record event, no matter how large or long standing, will eventually be broken (Glick 1978). Thus, the probability that the largest observed flood discharge on a river will be exceeded is 1, and this is true even if the flood's magnitude has an upper bound. However, we do not know the magnitude of the next record flood, other than that it will be greater than the current record flood, that is, the largest observed flood on record. Also, we do not know when the next record flood will occur. The same ideas apply to droughts, or to any other hydrologic flux. Other hydrologic records of interest might include the largest 24-hour rainfall on record, the lowest 7-day streamflow on record, the lowest value of soil moisture on record, and so on. Historically, engineers have always shown particular interest in such records. For example, most hydrology textbooks and manuals list record rainfall amounts that have occurred for various durations. Similarly, for flood discharges, envelope curves based on record floods have been drawn to bound our experience on floods for a particular region, and such curves have found widespread usage in engineering practice for the design of dams and other important facilities in the vicinity of rivers such as nuclear power plants. What is missing from our historical interest in hydrologic records is a theory that enables us to make probabilistic statements about their future occurrence. The purpose of this chapter is to provide such a theoretical framework for describing the probabilistic behavior of hydrologic record events.

The largest or smallest event exhibited within a sequence is a statistical property of a sequence that has long attracted the attention of hydrologists in dealing with floods and droughts through extreme value theory. However, study of record hydrologic events through the formal theory of records has only recently been undertaken, particularly studies of record floods. See [Vogel et al. \(2001\)](#) and [Castellarin et al. \(2005\)](#).

Surely all extraordinary floods are record floods, though not all record floods are extraordinary floods. What distinguishes an extraordinary flood from a flood of record, from a probable maximum flood, or from a 10,000-year flood? The theory of records can provide us with both a mathematical framework for dealing with such questions and a methodology for estimating the probability of occurrence associated with record floods. This chapter combines a theoretical framework for applying the theory of records to flood and other hydrologic processes, while simultaneously documenting numerous recent studies and approaches that have used the theory of records to assign probabilistic statements to extraordinary floods for the purpose of flood management and planning.

Since the pioneering work of [Chandler \(1952\)](#), a rich theory on the mathematics of record events has been developed leading to several summary texts ([Ahsanullah 1995, 2004](#); [Arnold et al. 1998](#); [Nevzorov 2001](#); [Arnold et al. 2008](#)). Within the context of the theory of order statistics, [Arnold et al. \(2008\)](#) provide a pedagogic treatment of the theory of records, suited for teaching the material in this chapter from the point of view of a mathematician. Mathematical interest in the theory of records seems to parallel general human interest in records, since the *Guinness Book of World Records* was first introduced in 1955. By 1974, the *Guinness Book of World Records* became the top-selling copyrighted book in publishing history and has become the authoritative source of records in nearly all fields of human and nonhuman endeavor ([Roberts 1991](#)).

The theory of records relies heavily upon the theory of order statistics ([David and Nagaraja 2003](#)) and extreme order statistics, as well as on the theory of extremes ([Gumbel 1958](#)). The theory of extremes has received a great deal of attention since its introduction by [Gumbel \(1958\)](#), with many advances occurring in the field of hydrology (see [Katz et al. 2002](#), for a recent overview of the field within the context of hydrology). Given the close association between the theory of records and water resource applications, surprisingly few water resource studies have applied the theory of records ([Vogel et al. 2001](#), [Nagaraja et al. 2003](#), [Castellarin et al. 2005](#), [Douglas and Vogel 2006](#), [Serinaldi and Kilsby 2018](#)).

Consider the following definition of record events. Let X_1, X_2, \dots, X_n represent a sequence of annual maximum (AM) flood observations, where n is the total number of time periods for which observations are available. The observation X_i is the n year record flood, which is denoted as Y , if X_i exceeds all previous records in the sequence of length n , or when $Y = \max(X_1, X_2, \dots, X_n)$. [Ahsanullah \(1995, 2004\)](#), [Arnold et al. \(1998, 2008\)](#), and [Nevzorov \(2001\)](#) introduce the entire upper record value sequence as follows. The observation X_j is called an upper record if $X_j > X_i$ for every $i < j$. The times at which these records occur are termed the record time sequence T_m , where the first observation is a record so that $T_0 = 1$, the second record occurs at time $t = j$, so that the record time is $T_1 = j$, and so on. The record value sequence is then $R_m = X_{T_m}$ where $m = 1, 2, \dots$. One can also define the interrecord time sequence as $\Delta_m = T_m - T_{m-1}$, $m = 1, 2, 3, \dots$. The number of upper records N_n in a series of n observations can also be tracked. For example, given the following sequence of $n = 6$ observations (50, 30, 60, 10, 80, 70), the upper record event is $Y = 80$, the resulting upper record time sequence ($T_0 = 1, T_1 = 3, T_2 = 5$), the resulting upper record value process ($R_1 = 50, R_2 = 60, R_3 = 80$), the interrecord time sequence [$\Delta_1 = T_1 - T_0 = 2, \Delta_2 = T_2 - T_1 = 2$], and the number of records in this series of $n = 6$ values is $N_n = 3$ records. All of these record value statistics apply to flood series and resulting flood management problems as described here.

The theory of records centers on probability distributions that are expressible in density, cumulative, and inverse closed forms. It is in this context that the adaptation of the theory of records to hydrologic studies is discussed. Note that in hydrologic studies, distributions expressible only in closed density form, such as the log-normal, and log-Pearson distributions, are used extensively, particularly in studies of floods. The theory of records does not per se exclude probability distributions that are not expressible in cumulative and inverse closed forms, but the current literature does not draw

attention to the use of simulation and Monte Carlo techniques to address properties of record events in terms of distributions that are not expressible in cumulative and inverse closed forms.

Much of the hydrologic literature assumes flood events are independent and identically distributed (*iid*). Interestingly, as we show in this chapter, much of the theory of records depends only on the *iid* assumption. Unfortunately, the *iid* assumption, underlying much of the theory of records, is hydrologically questionable. Though observations of flows lend some credence to the assumption of *iid* in the case of floods, the same cannot be said in reference to droughts. In the case of droughts, persistence, measured by serial correlation, is generally accepted and addressed primarily by assuming low flows are generated by stationary stochastic processes. The general acceptance of climate change by the scientific community has prompted increased attention in dealing with nonstationarity of hydrologic stochastic processes. It remains to be seen to what extent and in what manner properties of record events predicated on the assumption of *iid* would be affected by accounting for variations in the tail weights of probability distributions and nonstationarity. Arnold et al. (2008) briefly consider the case of “records in improved populations” for the case when the process of interest X , is stochastically ordered, so that the process is nonstationary.

This presentation of the theory of records follows the classical theory of record-breaking processes. Thus an objective frequency-based approach that assumes stationary extreme value processes is adopted. It is well documented in several places that the theory of records has a connection to both the theory of extremes and to the theory of order statistics. There are numerous recent developments in the theory of extremes and the theory of order statistics. Given that these three theories are connected, considering connections among extreme value theory, order statistics, record-breaking theory, and other complications due to nonstationarity, along with Bayesian-based statistical analyses, is important. It is anticipated that future work on record processes in hydrology will address these and other issues.

The following summarizes our current knowledge of the theory of record events, along with some new results directed to hydrologic studies. The chapter is broken into three sections: (1) parametric results, (2) nonparametric results, and (3) applications of the theory of record events to envelope curves. In the section on parametric results, we summarize the distributional properties of the flood of record Y and the entire upper record sequence R_m , corresponding to various commonly used probability distributions for X . In the section on nonparametric results, we summarize the statistical properties of the recurrence time (or return period) of the records Y and the nonparametric properties of record-breaking processes, such as the distribution of the number of records in an n year sequence termed N_n . The last section summarizes a few recent case studies that have applied the theory of records to estimate the exceedance probability associated with envelope curves and have tested the theory of records for evaluating the independence of flood records.

12.1 PARAMETRIC PROPERTIES OF HYDROLOGIC RECORDS

All statistical methods can be classified as either parametric or nonparametric. Parametric methods are generally based on an underlying assumption regarding the distribution of the random variable of interest, whereas nonparametric methods generally do not require such assumptions. For example, all of the expressions for the first two moments of X and Y for various assumed probability density functions (pdfs) given in Tables 12-1 and 12-2 are parametric results. Nonparametric methods tend to focus on the ranked or ordered observations because ordered observations have various theoretical properties that are independent of the distribution of the random variable of interest. In the following sections we review both parametric and nonparametric properties of record events.

12.1.1 The Probability Distribution, Quantile Function, and Moments of Record Floods

In this section we consider some probability distributions that arise in the theory of extremes (Beirlant et al. 2004) and are commonly used in flood frequency analysis, such as the exponential

Table 12-1. The Properties of the Random Variable X and Its Record Process Y for a Gumbel and a Generalized Extreme Value Distribution.

	Gumbel distribution	Generalized extreme value distribution
cdf of X	$F_X(x) = \exp\left\{-\exp\left(-\frac{(x-\xi)}{\alpha}\right)\right\}$	$F_X(x) = \exp\left(-\left[1 - \kappa \cdot \frac{(x-\xi)}{\alpha}\right]^{1/\kappa}\right)$ for $\kappa \neq 0$
Mean of X	$\mu_x = \xi + \gamma\alpha$	$\mu_x = \xi + \alpha[1 - \Gamma(1 + \kappa)]/\kappa$
Variance of X	$\sigma_x^2 = (\pi\alpha)^2/6$	$\sigma_x^2 = \alpha^2\{\Gamma(1 + 2\kappa) - [\Gamma(1 + \kappa)]^2\}/\kappa^2$
Quantile of X	$x(p_x) = \xi - \alpha \ln(-\ln(p_x))$	$x(p_x) = \xi + \frac{\alpha}{\kappa} \left[1 - (-\ln(p_x))^\kappa\right]$
Quantile of Y	$y(p_y) = \xi - \alpha \ln\left(-\frac{\ln(p_y)}{n}\right)$	$y(p_y) = \xi + \frac{\alpha}{\kappa} \left[1 - \left(-\frac{\ln(p_y)}{n}\right)^\kappa\right]$
Mean of Y	$\mu_y = \xi + \alpha(\gamma + \ln(n))$ $= \mu_x + \alpha \ln(n)$	$\mu_y = \xi + \frac{\alpha}{\kappa} \left[1 - \frac{\Gamma(1+\kappa)}{n^\kappa}\right]$
Variance of Y	$\sigma_y^2 = \sigma_x^2 = \frac{\pi^2\alpha^2}{6}$	$\sigma_y^2 = \left(\frac{\alpha}{\kappa \cdot n^\kappa}\right)^2 \{\Gamma(1 + 2\kappa) - [\Gamma(1 + \kappa)]^2\}$

Note: cdf = cumulative density function.

Table 12-2. Properties of the Random Variable X and Its Record Process Y for the Exponential and Generalized Pareto Distributions.

	Exponential distribution	Generalized pareto distribution
cdf of X	$F_X(x) = 1 - \exp(-\beta(x - \xi))$	$F_X(x) = 1 - [1 - \beta(x - \xi)]^{1/\kappa}$
Mean of X	$\mu_x = \xi + (1/\beta)$	$\mu_x = \xi + [1/(\beta(1 + \kappa))]$
Standard deviation of X	$\sigma_x = 1/\beta$	$\sigma_x = (1/\beta) \sqrt{\Gamma[1 + (2/\kappa)] - \Gamma^2[1 + (1/\kappa)]}$
Quantile of X	$x(p_x) = \xi - (\ln(1 - p_x))/\beta$	$x(p_x) = \xi + [1 - (1 - p_x)^\kappa]/(\kappa\beta)$
Quantile of Y	$y(p_y) = \xi - \frac{\ln(1-p_y^{1/n})}{\beta}$	$y(p_y) = \xi - \frac{(1-p_y^{1/n})^\kappa}{\beta \cdot \kappa}$
Mean of Y	$\mu_y = \xi + \frac{1}{\beta} \sum_{v=1}^n \frac{1}{v}$	Not available
Variance of Y	$\sigma_y^2 = \frac{1}{\beta} \sum_{v=1}^n \frac{1}{v^2}$	Not available

Note: cdf = cumulative density function.

(EXP) and generalized Pareto (GPA) distributions used in the analysis of flood peaks over a threshold (POT), and the Gumbel (GUM) and generalized extreme value (GEV) distributions used for modeling AM flood series. Further, we only consider exact results, so that in instances when only asymptotic results are available, we do not report them, because in the field of hydrology flood samples are usually not nearly long enough for asymptotic results to apply. We begin by summarizing the pdf, cumulative density function (cdf), quantile function, and moments (where possible) of a record flood drawn from these distributions and the moments of the record process R_m .

Suppose the *iid* annual maximum flood series X has a known cdf $F_X(x)$. The cdf for the record flood Y is then

$$F_Y(y) = [F_X(y)]^n \quad (12-1)$$

where n is the length of the series of annual maximum floods. Similarly, the pdf of Y can be obtained by differentiation of Equation (12-1):

$$f_Y(y) = dF_Y(y)/dy \quad (12-2a)$$

or in terms of the original pdf and cdf of X (Ang and Tang 1984):

$$f_Y(y) = n[F_X(y)]^{n-1}f_X(y) \quad (12-2b)$$

All of the extreme value pdfs considered here have quantile functions that can be expressed analytically, hence we found it useful to derive moments of Y using the fact that

$$\mu_r = \int_0^1 y^r(p) dp \quad (12-3)$$

where μ_r denotes the r^{th} moment of Y about the origin, and $p = F_Y(y)$ and $y(p)$ are the quantile functions of the record floods Y . The quantile function is also sometimes referred to as the inverse of the cdf. All the results in the following section regarding the properties of Y are derived from Equations (12-1)–(12-3).

We begin by summarizing the properties of record floods drawn from GUM and GEV distributions, followed by a summary of the properties of record floods drawn from EXP and GPA distributions. Further details on all four of these distributions, including their product moments, L-moments, parameter estimators, and goodness-of-fit tests, can be found in Hosking and Wallis (1997) and Stedinger et al. (1993). Gumbel (1958) provides a comprehensive treatment of the GUM and EXP distributions.

12.1.2 The Gumbel Distribution

If X arises from a GUM distribution, then its cdf is

$$F_X(x) = \exp\left\{-\exp\left(-\frac{(x-\xi)}{\alpha}\right)\right\} \quad (12-4)$$

where ξ is the location parameter and α is the scale parameter. The location parameter ξ is equal to the mode of x , which can be determined by setting $df_x(x)/dx = 0$ and solving for $x_{\text{mode}} = \xi$ where $f_x(x) = dF_x(x)/dx$. The mean and variance of X are $\mu_x = \xi + \gamma\alpha$ and $\sigma_x^2 = (\pi\alpha)^2/6$ respectively, where $\gamma = 0.5772$ is the Euler number. The quantile function of a GUM variable is given by

$$x(p_x) = \xi - \alpha \ln(-\ln(p_x)) \quad (12-5)$$

where $p_x = F_X(x)$. The range of x in Equations (12-4) and (12-5) is unbounded both above and below so that $-\infty < x < \infty$.

Substitution of Equation (12-4) into Equations (12-1) and (12-2) leads to the cdf and pdf of the record flood series Y generated from GUM samples of length n . Inversion of the cdf of Y leads to the quantile function for the record flood Y drawn from a GUM sample of length n :

$$y(p_y) = \xi - \alpha \ln\left(-\frac{\ln(p_y)}{n}\right) = \xi - \alpha \ln(-\ln(p_y)) + \alpha \ln(n) \quad (12-6)$$

where $p_y = F_Y(y) = F_X(y)^n$. Note that the quantile functions of the Y series and the X series differ only by the constant term $\alpha \ln(n)$, and for the special case when $n = 1$, the quantile function of the Y series is identical to the quantile function for the X series in Equation (12-5). Therefore, if the distribution of annual maximum floods follows a GUM distribution, the distribution of the record

flood Y will also be Gumbel. This is consistent with the findings of Gumbel (1958), Ang and Tang (1984), Lambert and Li (1994), and others.

Exact expressions for the mean, μ_y , and variance, σ_y^2 , of record floods drawn from a GUM series of length n were first introduced by Gumbel (1958) and may be derived by substitution of Equation (12-6) into Equation (12-3) and using the fact that $\mu_y = \mu_1$ and $\sigma_y^2 = \mu_2 - \mu_1^2$, leading to

$$\mu_y = \xi + \alpha(\gamma + \ln(n)) = \mu_x + \alpha \ln(n) \quad (12-7a)$$

$$\sigma_y^2 = \sigma_x^2 = \frac{\pi^2 \alpha^2}{6} \quad (12-7b)$$

where $\gamma = 0.5772$ is the Euler number. As expected, all moments of Y reduce to the moments of X when $n = 1$, and Y always has exactly the same variance as X , regardless of n . Because both X and Y are Gumbel, they also both have skewness of 1.1396. Arnold et al. (1998, Equations 2.7.15 and 2.7.16) also report the mean and variance of Y ; however, their expressions were found to be in error because they do not reduce to the moments of X when $n = 1$, nor do they reproduce the expected moments when we performed Monte Carlo experiments to check Equation (12-7). The mode of Y , also given by Gumbel (1958), is easily derived by setting $df_y(y)/dy = 0$ and solving for y , where $f_y(y)$ is given by Equation (12-2), resulting in

$$y_{mode} = \xi + \alpha \ln(n) \quad (12-8a)$$

Thus, the mean record event μ_y is always greater than its mode y_{mode} by an amount equal to $\gamma\sigma_x\sqrt{6}/\pi = 0.45\sigma_x = 0.45\sigma_y$. Similarly, the mean of x is also always greater than its mode by the same amount, $0.45\sigma_x$. Gumbel (1958) also reports the median of Y as

$$y(0.5) = \xi + \alpha(0.36651 + \ln(n)) \quad (12-8b)$$

which always lies between the mode and mean. Figure 12-1 compares the exceedance probability $[1 - F_x(\bar{y})]$ of the mean $\bar{y} = \mu_y$, median $y(0.5)$, and mode y_{mode} of y with the expected exceedance probability $1/(n+1)$, illustrating that all three measures of central tendency of the flood of record y tend to be exceeded more frequently than one would expect, on average, for a given sample size n . Note that the sample estimator of the nonexceedance probability of the i^{th} observation in a sample ordered in ascending order, $i/(n+1)$, known as the Weibull plotting position, yields unbiased

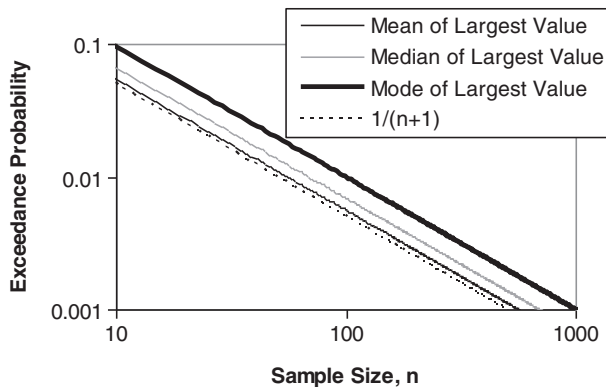


Figure 12-1. Exceedance probability of various measures of central tendency associated with the flood of record from a Gumbel distribution.

estimates of the exceedance probability of any random variable, regardless of its underlying distribution.

L-moments are often preferred over ordinary moments, for parameter estimation and goodness-of-fit evaluation (Hosking and Wallis 1997, Stedinger et al. 1993). The first L-moment of Y is equal to the first ordinary moment of Y given in Equation (12-7a). The second L-moment of Y , denoted $\lambda_2(y)$, is identical to the second L-moment of X , denoted $\lambda_2(x)$, which are both given by

$$\lambda_2(y) = \lambda_2(x) = \alpha \ln(2) \quad (12-9)$$

The L-skew of both X and Y is equal to 0.1699, and the L-kurtosis of both X and Y is equal to 0.1504.

Arnold et al. (1998) document that the upper record process (i.e., the time sequence of record events in a series of extremes; see Section 12.1) for the case when X follows a Gumbel pdf is defined by

$$R_m = \xi + \alpha \ln(R_m^*) \quad (12-10)$$

where R_m^* is a gamma $(m+1, 1)$ random variable, so that the mean and variance of the upper record process is given by

$$E[R_m] = \xi - \alpha\gamma + \alpha \sum_{j=1}^m \frac{1}{j} \quad (12-11)$$

$$Var[R_m] = \alpha^2 \left[\frac{\pi^2}{6} - \sum_{j=1}^m \frac{1}{j^2} \right] \quad (12-12)$$

where again $\gamma = 0.5772$ is the Euler number.

12.1.3 The Generalized Extreme Value Distribution

Douglas and Vogel (2006) first derived the cumulative distribution function, quantile function, moments, and L-moments of the record floods Y for the case when the flood series X_i follows a GEV distribution. The origins of the GEV distribution can be traced to a paper by Fisher and Tippett (1928), which seems to be the first account of what today is referred to as the GEV model. Later the GEV model was discussed by Mises (1936) and subsequently applied by Jenkinson (1955) and is now perhaps the most widely accepted distribution for modeling flood series in the world (see Table 1 of Vogel and Wilson 1996). Its cdf is

$$F_X(x) = \exp\left(-\left[1 - \kappa \cdot \frac{(x - \xi)}{\alpha}\right]^{1/\kappa}\right) \quad \text{for } \kappa \neq 0 \quad (12-13)$$

where ξ is the location parameter, α is the scale parameter, and κ is the shape parameter (Jenkinson 1955). As the shape parameter κ approaches zero, the GEV distribution approaches a GUM (or extreme value type I) distribution. The mean and variance of x are given by $\mu_x = \xi + \alpha[1 - \Gamma(1 + \kappa)]/\kappa$ and $\sigma_x^2 = \alpha^2\{\Gamma(1 + 2\kappa) - [\Gamma(1 + \kappa)]^2\}/\kappa^2$. The range of x in Equation (12-13) is $-\infty < x < \xi + \frac{\alpha}{\kappa}$ for $\kappa > 0$ and $\xi + \frac{\alpha}{\kappa} \leq x < \infty$ for $\kappa < 0$, so that both X and Y will have an upper bound when $\kappa > 0$, as Enzel et al. (1993) and others suggest. Chowdhury et al. (1991) provide goodness-of-fit tests and hypothesis tests for the GEV distribution.

The quantile function for the original flood series X is obtained by solving Equation (12-13) for x which yields

$$x(p_x) = \xi + \frac{\alpha}{\kappa} [1 - (-\ln(p_x))^\kappa] \quad (12-14)$$

where $p_x = F_X(x)$. Substitution of Equation (12-13) into Equations (12-1) and (12-2) leads to the cdf and pdf of the record flood series Y generated from GEV samples of length n . The inverse distribution of Y leads to the quantile function for the record flood Y , drawn from a GEV sample of length n :

$$y(p_y) = \xi + \frac{\alpha}{\kappa} \left[1 - \left(\frac{-\ln(p_y)}{n} \right)^\kappa \right] \quad (12-15)$$

where $p_y = F_Y(y) = F_X(y)^n$. When $n = 1$, the quantile function of Y in Equation (12-15) reduces to the quantile function for the X series in Equation (12-14). Note that Equation (12-15) is similar in form to the quantile function for the original GEV variate X , given in Equation (12-14). Douglas and Vogel (2006) use the quantile function in Equation (12-14) to derive the moments and L-moments of Y when X arises from a GEV pdf. The mean, μ_y , and variance, σ_y^2 , of Y are

$$\mu_y = \xi + \frac{\alpha}{\kappa} \left[1 - \frac{\Gamma(1 + \kappa)}{n^\kappa} \right] \quad (12-16a)$$

$$\sigma_y^2 = \left(\frac{\alpha}{\kappa \cdot n^\kappa} \right)^2 \{ \Gamma(1 + 2\kappa) - [\Gamma(1 + \kappa)]^2 \} \quad (12-16b)$$

Similar to the quantile function, the first two moments of Y differ in form from those of X , only by the additional term, n^κ . Figure 12-2 compares the exceedance probability $[1 - F_x(\mu_y)]$ of the mean record flood from a GEV distribution, for various values of the shape parameter, with the expected exceedance probability $1/(n + 1)$. Figure 12-2 documents that the mean record flood (in real space) from a GEV distribution tends to be exceeded less frequently than one would expect for a given sample size n when the shape parameter is negative.

The first L-moment of Y is identical to the mean of Y in Equation (12-16a). The second L-moment of Y is

$$\lambda_2(y) = \frac{\alpha \Gamma(1 + \kappa)}{\kappa n^\kappa} (1 - 2^{-\kappa}) \quad (12-17)$$

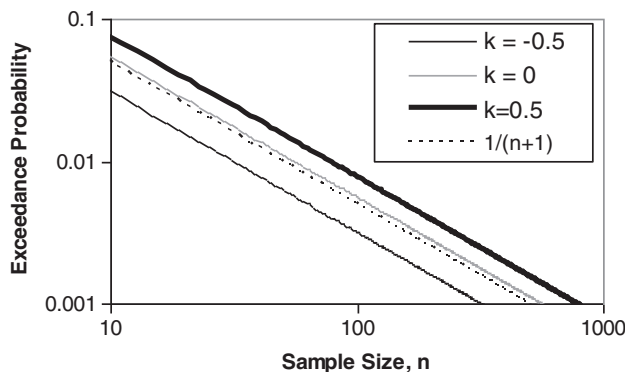


Figure 12-2. Exceedance probability of the mean flood of record μ_y from a GEV distribution for various values of the shape parameter.

The mode of Y is easily derived by setting $df_y(y)/dy = 0$ and solving for y , where $f_y(y)$ is given by Equation (12-2), resulting in

$$y_{\text{mode}} = \xi + \frac{\alpha}{\kappa} \left[1 + \left(\frac{\kappa - 1}{n - \kappa} \right)^{\kappa} \right] \quad (12-18)$$

The L-skew and L-kurtosis of Y are the same as for the original X series given by Stedinger et al. (1993), Hosking and Wallis (1997), and others. Thus, if X follows a GEV distribution, then Y is also GEV with the same shape parameter κ . Only their means and coefficients of variation differ. We are unaware of any previous work summarizing the pdf or moments of the upper record process for the GEV case, analogous to the results for the Gumbel distribution in Equations (12-10)–(12-12).

12.1.4 The Exponential Distribution

For an AM series of floods distributed as a GUM distribution, Stedinger et al. (1993) and others show that the POT flood series will follow an EXP distribution with pdf, cdf, and quantile function given by $f_X(x) = \beta \exp(-\beta(x - \xi))$, $F_X(x) = 1 - \exp(-\beta(x - \xi))$, and $x(p_x) = \xi - (\ln(1 - p_x)/\beta)$, respectively, with mean and standard deviation given by $\mu_x = \xi + (1/\beta)$ and $\sigma_x = 1/\beta$, respectively. Here ξ is generally the threshold value above which flood peaks are reported, hence it is given or assumed, along with the flood series. Substitution of the EXP cdf into Equation (12-1) yields the cdf of the maximum value, which is easily inverted to obtain the quantile function of the record flood for an EXP variable:

$$y(p_y) = \xi - \frac{\ln(1 - p_y^{1/n})}{\beta} \quad (12-19)$$

where $p_y = F_Y(y)$. Gumbel (1958) and Arnold et al. (1998) report exact expressions for the mean and variance of Y (as well as other properties) when X arises from a standard exponential distribution that assumes $\xi = 0$ and $\beta = 1$. Those expressions can be generalized for the exponential distribution introduced here, leading to expressions for the mean and variance of the record flood:

$$\mu_y = \xi + \frac{1}{\beta} \sum_{v=1}^n \frac{1}{v} \quad (12-20a)$$

$$\sigma_y^2 = \frac{1}{\beta^2} \sum_{v=1}^n \frac{1}{v^2} \quad (12-20b)$$

Raqab (2004) derives recurrence relations for the moments of order statistics from a generalized EXP distribution. Numerical integration also provides exact estimates of the moments of Y by substitution of Equation (12-19) into Equation (12-3). Parameter estimates ξ and β obtained from the X series may be used in Equation (12-19) to generate series of record floods or to characterize the pdf or cdf of the Y series using Equations (12-1) and (12-2).

12.1.5 Generalized Pareto Distribution

In the case where an AM series of floods follows a GEV distribution, Stedinger et al. (1993) and others show that the POT flood series follows a GPA distribution with pdf, cdf, and quantile function given by $f_X(x) = \beta[1 - \exp(-\kappa\beta(x - \xi))]^{(1-\kappa)/\kappa}$, $F_X(x) = 1 - [1 - \beta(x - \xi)]^{1/\kappa}$, and

$x(p_x) = \xi + [1 - (1 - p_x)^\kappa]/(\kappa\beta)$, respectively, with the mean and standard deviation given by $\mu_x = \xi + [1/(\beta(1 + \kappa))]$ and $\sigma_x = (1/\beta)\sqrt{\Gamma[1 + (2/\kappa)] - \Gamma^2[1 + (1/\kappa)]}$. Here again, ξ is the threshold value above which flood peaks are reported. Applying Equation (12-1) to the GPA cdf yields the cdf of Y , which is easily inverted to obtain the quantile function of the record flood for a GPA process:

$$y(p_y) = \xi - \frac{(1 - p_y^{1/n})^\kappa}{\beta\kappa} \quad (12-21)$$

where $p_y = F_Y(y)$. Balakrishnan and Ahsanullah (1994) derive recurrence relations for the moments of order statistics for a GPA distribution, but we were unable to obtain closed-form solutions to either the moments or L-moments of Y for the GPA distribution. Arnold et al. (1998) report exact expressions for the mean and variance of Y when X arises from a Pareto model, which is parameterized quite differently from the GPA model. Numerical integration provides exact estimates of the moments of Y by substitution of Equation (12-21) into Equation (12-3). Estimates of ξ , κ , and β obtained from the X series may be used in Equation (12-21) to generate series of record floods or to characterize the pdf or cdf of the Y series using Equation (12-1) and Equation (12-2).

Tables 12-1 and 12-2 summarize the parametric properties of hydrologic records.

12.2 NONPARAMETRIC STATISTICAL PROPERTIES OF HYDROLOGIC RECORDS

For a discussion of the distinction between parametric and nonparametric approaches to summarizing the statistical properties of hydrologic records, see Section 12.1.

12.2.1 The Recurrence or Waiting Time of Record Floods

Interestingly Wilks (1959) and Gumbel (1961) show that the probability distribution of the unconditional waiting or recurrence time to the next record flood has no moments, thus other measures are needed to define the waiting time to the next record flood. That this important yet paradoxical result has received so little attention in the water resources literature is surprising. The only publication we could find in the field of water resources that cited either of these papers is Castellarin et al. (2005). Chandler (1952) and Gumbel (1961) give the pdf of the waiting time T to exceed the m^{th} largest observation in a sample of size n as

$$f_T(t) = \binom{n}{m} m t^{-m-1} \left(1 - \frac{1}{t}\right)^{n-m} \quad \text{for } t \geq 1 \quad (12-22)$$

For example, the expected value of the waiting time T is given by $E[T] = n/(m-1)$, which is clearly infinite for the record flood ($m = 1$), but finite for all other order statistics. Similarly, all upper moments of T corresponding to the record flood are infinite.

Equation (12-22) written from $m = 1$ gives the pdf of the waiting time to exceed the record flood, which yields

$$f_T(t) = \frac{n}{t^2} \left(1 - \frac{1}{t}\right)^{n-1} \quad \text{for } t \geq 1 \quad (12-23)$$

Figure 12-3 illustrates the pdf of the recurrence time for the three cases $n = 10, 50$, and 100 .

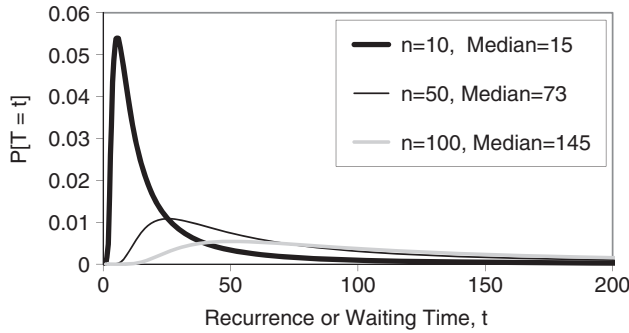


Figure 12-3. Probability distribution of the recurrence time to the next record flood for a sample of size $n = 10, 50$, and 100 years, after just having observed a record flood.

Gumbel (1961) also gives the cdf of the waiting time to exceed the record flood as

$$F_T(t) = \left(1 - \frac{1}{t}\right)^n \quad (12-24)$$

The quantile function for the waiting time to exceed the record flood is easily obtained from Equation (12-24) as

$$T(p) = \frac{1}{1 - p^{1/n}} \quad (12-25)$$

where $p = F_T(t)$.

In addition to the expectation of the recurrence time of the record flood, other measures of central tendency such as the mode, median, and geometric mean of the recurrence time exist for the record flood. Because the moments of the recurrence times do not exist, one could use the mode, median, quantiles, and possibly upper L-moments to describe the recurrence time of the record flood distribution in lieu of the moments.

Gumbel (1961) gives the geometric mean T_G , median T_{median} , and mode T_{mode} of the waiting time to the next record flood as

$$T_G = \exp \left[\sum_{j=1}^n \frac{1}{j} \right] \cong \gamma + \ln(n) = 1.78n \quad (12-26)$$

$$T_{median} = \frac{2^{1/n}}{(2^{1/n} - 1)} \cong \frac{n}{\ln(2)} + \frac{1}{2} = 1.44n + 0.5 \quad (12-27)$$

$$T_{mode} = \frac{n+1}{2} \quad (12-28)$$

Note that in general $T_{mode} < n < T_{median} < T_G$. Clearly these measures of central tendency of the waiting time to the next record flood vary over a significant range from roughly $0.5n$ to $1.8n$.

12.2.2 The Probability Distribution of the Number of Record Events

The time of occurrence at which record highs occur in the original sequence may be expressed as the series of binary variates:

$$Y_i = \begin{cases} 1 & \text{if } X_i = \max(X_1, X_2, \dots, X_i) \\ 0 & \text{otherwise} \end{cases} \quad (12-29)$$

Let R denote the number of record-breaking events in an n year period where

$$R = \sum_{i=1}^n Y_i \quad (12-30)$$

If the *max* function in Equation (12-29) is replaced by *min*, one obtains the lower record events. Alternatively, one can switch from upper- to lower-record events, by replacing the original sequence with $-X_1, -X_2, \dots, -X_n$. Some initial theoretical results are taken from the mathematics literature, and others are introduced here for the first time.

David and Barton (1962) first introduce an expression, using Stirling numbers, for the exact probability mass function (pmf) for the number of upper- and lower-record events in an n year period. A much simpler yet identical expression for the exact pmf of R , denoted $P_n[R=r]$ (see Vogel et al. 2001), is defined by the recursion

$$P_j[R=r] = \left(1 - \frac{1}{j}\right) P_{j-1}[R=r] + \left(\frac{1}{j}\right) P_{j-1}[R=r-1] \quad (12-31)$$

for $r \geq 1$ and $j \geq 2$ with the initial values $P_1[R=0] = 0$ and $P_1[R=1] = 1$. Glick (1978) also reports the asymptotic result for large sample sizes:

$$P_n[R=r] = \frac{[\ln(n)]^{r-1}}{n \cdot (r-1)!} \quad (12-32)$$

Combining the definition of the cmf $P[R \leq r] = \sum_{k=1}^r P[R=k]$ with the asymptotic result in Equation (12-32), and after algebra, we obtain

$$P[R \leq r] = \frac{\Gamma(r, \ln(n))}{\Gamma(r)} \quad (12-33)$$

where $\Gamma(x, y)$ is the incomplete gamma function defined by $\Gamma(a, b) = \int_b^\infty t^{a-1} e^{-t} dt$. Note that the gamma function is a special case of the incomplete gamma function whereby $\Gamma(a) = \Gamma(a, 0)$. Figure 12-4 illustrates the agreement between the asymptotic approximation of the cmf and the exact result for $n = 10$ and 100. We recommend the use of the exact result.

12.2.3 Moments of the Number of Record-Breaking Events

The first observation is defined to be a record event. The following results for the mean and variance of R are due to Glick (1978):

$$\mu_R = \sum_{i=1}^n 1/i \quad (12-34)$$

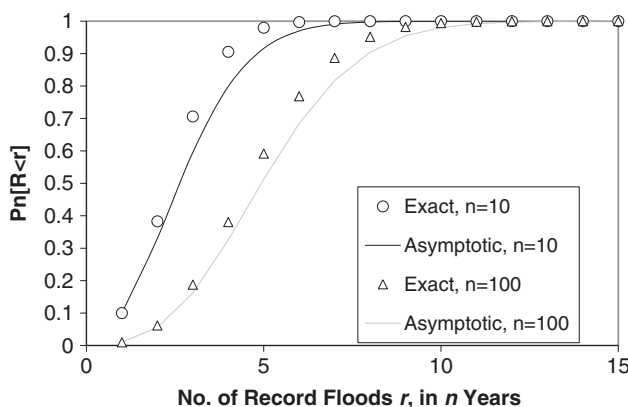


Figure 12-4. Comparison of exact and asymptotic cmfs for the number of record floods in 10- and 100 year periods.

and

$$\sigma_R^2 = \sum_{i=1}^n 1/i - \sum_{i=1}^n 1/i^2 \quad (12-35)$$

Zafirakou-Koulouris (2000, p. 26) derived an exact expression for the skewness of R :

$$\gamma_R = \frac{\sum_{i=1}^n 1/i - 3 \sum_{i=1}^n 1/i^2 + 2 \sum_{i=1}^n 1/i^3}{\left(\sum_{i=1}^n 1/i - \sum_{i=1}^n 1/i^2 \right)^{3/2}} \quad (12-36)$$

as well as an approximation to the kurtosis of R

$$\kappa_R \cong 3.19 - \frac{1.42}{n} - \frac{5.43}{n^2} - 0.00419\sqrt{n} \quad (12-37)$$

The approximation in Equation (12-37) is accurate to at least three decimal places for $4 \leq n \leq 100$.

Vogel et al. (2001) use moment diagrams based on Equations (12-34) to (12-37) to show that in spite of the central limit theorem, the tail behavior of the distribution of R differs significantly from other common distributions even for large sample sizes. Among distribution functions commonly used, the distribution of R closely resembles the normal distribution, though only approximately. Table 12-3 summarizes the moments and moment ratios of the number of record-breaking events in a series of length n .

12.2.4 Multivariate Record Events

Hydrologists have a long-standing and continuing interest in reducing the sampling errors associated with the estimates of specific statistical properties of hydrologic sequences, for example, the parameters of distributions presumed to provide a good probabilistic description of the sequences, or more generally, the moments of the distributions determined from the sequences. Achieving reduction in sampling error via the transfer of information from sequences at nearby sites to a sequence at a particular site is referred to as regionalization, which is a means of augmenting time averages through spatial averages. Collectively the sites comprise a region. Techniques of

Table 12-3. Moments and Moment Ratios of the Number of Record Breaking Events, R .

Moment or moment ratio	Theoretical expression
Mean	$\mu_R = \sum_{i=1}^n \frac{1}{i}$
Variance	$\sigma_R^2 = \sum_{i=1}^n \frac{1}{i} - \sum_{i=1}^n \frac{1}{i^2}$
Skewness	$\gamma_R = \left(\sum_{i=1}^n \frac{1}{i} - 3 \sum_{i=1}^n \frac{1}{i^2} + 2 \sum_{i=1}^n \frac{1}{i^3} \right) / \left(\sum_{i=1}^n \frac{1}{i} - \sum_{i=1}^n \frac{1}{i^2} \right)^{3/2}$
Kurtosis	$\kappa_R = 3.19 - 1.42 \frac{1}{n} - 5.43 \frac{1}{n^2} - 0.00419 \sqrt{n}$
Coefficient of variation	$C_v(R) = \sqrt{\sum_{i=1}^n \frac{1}{i} - \sum_{i=1}^n \frac{1}{i^2} / \sum_{i=1}^n \frac{1}{i}}$

regionalization must contend with the structure of dependence exhibited by the set of m regional sequences. In the following discussions, the lengths of the sequences are assumed to be the same, n , at all sites unless otherwise noted. Further assumed is that the sequences are realizations of a stationary multivariate stochastic process.

The dependence structure may be expressed in terms of the matrix of pairwise product-moment correlations between the sequences:

$$R = \begin{bmatrix} 1 & r_{1,2} & r_{1,3} & r_{1,4} & r_{1,m} \\ r_{2,1} & 1 & r_{2,3} & r_{2,4} & r_{2,m} \\ r_{3,1} & r_{3,2} & 1 & r_{3,4} & r_{3,m} \\ r_{4,1} & r_{4,2} & r_{4,3} & 1 & r_{4,m} \\ r_{m,1} & r_{m,2} & r_{m,3} & r_{m,4} & 1 \end{bmatrix} \quad (12-38)$$

As is well known, R is a symmetric matrix: $r_{j,k} = r_{k,j}$, $\forall j, k$, and $r_{j,k} = 1$ for $j = k$, where $r_{j,k} \rightarrow \rho_{j,k}$ as $n \rightarrow \infty$. If $r_{j,k}(\rho_{j,k}) = 0$ and $\forall j \neq k$, then $R \equiv I$, where I is the identity matrix. In general, the effectiveness of regionalization in transferring information to a site of interest from nearby sites diminishes as $\rho_{j,k} \rightarrow 1$. The univariate probability distributions describing the sequences at each of the m sites are the marginal distributions of the multivariate distribution defining the structure of dependence between the m sequences.

Little hydrologic attention has been directed to multivariate distributions, apart from the multivariate normal distribution, in particular the bivariate normal distribution. Among recent publications on multivariate distributions in hydrology are Kallache et al. (2013), Bardossy and Horning (2016), and Salvadori et al. (2016). Transformations of hydrologic sequences to provide better descriptions by specific univariate distributions do not ensure that a multivariate distribution having those univariate distributions as its marginal distributions will satisfactorily describe the sequences collectively. Multivariate normal distributions have normal marginal distributions, but multivariate distributions other than multivariate normal distributions may have nonnormal marginals. Moreover, product moment correlations are not invariant to transformation.

Flood experience is often summarily reported in terms of flood envelope curves as suggested by Jarvis (1926). The record floods at sites within a specified region, paired with the drainage areas at the sites, are plotted relative to a specified enveloping line, that is, a line below which all paired points lie. The enveloping line is a basis of regionalization, as the line is defined by the flood experience as a function of drainage area at the various sites. The probability that a flood at a specific site will exceed the flood defined by the envelope line for that site provides a regional basis for assessing the flood risk at that site. The probability of exceeding the envelope line at a particular site depends upon the degree of dependence among the record floods at the regional sites, and that dependence is a

function of the dependence structure of the sequences from which the record floods are derived and upon the length of the sequences. However, the dependence between sequences is not a major determinant, as that correlation tends to zero as the length of the sequences increases.

The dependence among the record flows may be expressed by the symmetric matrix of the product-moment correlations between the record flows:

$$W = \begin{bmatrix} 1 & w_{1,2} & w_{1,3} & w_{1,4} & w_{1,m} \\ w_{2,1} & 1 & w_{2,3} & w_{2,4} & w_{2,m} \\ w_{3,1} & w_{3,2} & 1 & w_{3,4} & w_{3,m} \\ w_{4,1} & w_{4,2} & w_{4,3} & 1 & w_{4,m} \\ w_{m,1} & w_{m,2} & w_{m,3} & w_{m,4} & 1 \end{bmatrix} \tag{12-39}$$

If $|\rho_{j,k}| < 1$ and $\forall j \neq k$, then

$$\lim_{n \rightarrow \infty} W \rightarrow I \tag{12-40}$$

where I denotes the identity matrix—the correlation between record values is asymptotically zero. If $|\rho_{j,k}| = 1$, then $|w_{j,k}| = 1$ and $\forall j,k$. See [Sibuya \(1960\)](#) and [Husler and Reiss \(1989\)](#). Two general properties of the distribution of record events within sequences are suggestive of Equation (12-40). First, record events tend to be sparsely distributed over a sequence. For example, from Equations (12-34) and (12-35), the expected number of records in sequences of length $n = 10$ is approximately 2.93 with standard deviation equal to about 1.17. For $n = 10^6$, the mean number of record events is about 14.39 with standard deviation equal to about 3.57. See, for example, [Glick \(1978\)](#). Second, record events tend to occur early in a sequence. Unlike the correlation between sequences that can be estimated directly from the sequences, the correlation between records must be inferred from the $r_{j,k}$ given the lengths of the sequences, n .

In an unpublished manuscript, Matalas and Olsen (personal communication) provided values of w corresponding to values of ρ and n . Table 12-4 illustrates that given ρ , w decreases as n increases. As ρ increases, w decreases at a slower rate as n increases. The correlations between record events reported by Matalas and Olsen were obtained via simulation of bivariate normal sequences of length n , $\{x_t : t = 1, \dots, n\}$, and $\{y_t : t = 1, \dots, n\}$:

$$x_t = \varepsilon_t \tag{12-41a}$$

$$y_t = \rho \varepsilon_t + \sqrt{1 - \rho^2} \delta_t \tag{12-41b}$$

where $\forall t$, x_t , y_t , ε_t , and δ_t are each distributed as $N(0, 1)$, and ε_t and δ_t are mutually independent. For each specified value of the couple (ρ, n) , $M = 50,000$ paired sequences $\{x\}$ and $\{y\}$ were generated, and from each of the paired sequences, the record values of the sequences were obtained. The correlation w was given by the correlation between the $M = 50,000$ paired record values.

Table 12-4. Correlation Between Records, w , Corresponding to Correlation Between Sequences, ρ , Given n .

$n \backslash \rho$	0.1	0.2	0.4	0.6	0.8	0.9
50	0.009	0.028	0.099	0.238	0.490	0.690
100	0.014	0.027	0.080	0.200	0.446	0.657
200	0.004	0.013	0.055	0.159	0.395	0.616

In a real-world context, the relation between w and ρ given n may be viewed in terms of Walker's (1999) partition of 423 sites in the United States into three regions, an eastern region consisting of 189 sites, a midwestern region consisting of 120 sites, and a western region consisting of 114 sites. At each site, sequences of annual floods were of length $n = 50$. The average correlations, \bar{r} , among the sequences were 0.212 for the eastern region, 0.177 for the midwestern region, and 0.420 for the western region. Under the assumption that floods at a given site are independently and identically distributed, the mean correlations between the record floods, \bar{w} , inferred from the \bar{r} 's, are 0.03 in the eastern region, less than 0.03 in the midwestern region, and about 0.10 in the western region.

If the number of sites in a region is M , the mean distance between the sites would increase as the area of the region increases, and the mean correlation between the sequences would decrease. In a small region where the distances between the sites are small, the correlation between sequences would tend to be large. Orographic effects on meteorological attributes of a region would render the mean correlation between the sequences smaller than they would be in the absence of those effects, whatever the area of the region may be. Moreover, if the length of each of the M sequences is n , the correlations between the sequences would be less if the sequences are nonconcurrent than if the sequences are concurrent. Thus, in general hydrologic settings of orographic effects and nonconcurrency of sequences, the mean correlation between record events would be smaller than they would otherwise be if the orographic effects were absent and if the sequences were all concurrent.

In the previous discussions, the dependence between sequences and the dependence between the record events within the sequences were expressed in terms of the correlations between the sequences and between the record events. Dependence is defined by the multivariate distribution underlying the m regional sequences. Unless dependence is linear, correlation may grossly misrepresent the degree of dependence. If the marginal distributions associated with the m dimensional distribution function for the region are assumed to be of a certain form, then the correlations purporting to define the degree of dependence between sequences may not be able to attain their full mathematical range $(-1, 1)$. For example, the marginal distributions of the bivariate Farlie-Gumbel-Morgenstern distribution yield a dependence structure marked by $|\rho| < 1/3$, whatever the marginal distributions are. Schucany et al. (1978) give the upper bound on $|\rho|$ for various marginal distributions, and Butkiewicz and Hys (1977) give a detailed account of the dependence structure in the case of Weibull marginal distributions of the bivariate Farlie-Gumbel-Morgenstern distribution and of its multivariate extension.

Bivariate distributions, such as the Farlie-Gumbel-Morgenstern distribution, for which the dependence structure is marked by correlations considerably less than their full mathematical range, have limited hydrologic utility because the distribution is itself limited to accommodating absolute values of cross-correlations equal to or less than $1/3$. However, such distributions are potentially useful in dealing with situations of low-level dependence structure, situations that arise in studies of regions of large spatial scope. In reference to the record events within sequences, the dependence structure tends to low-level dependence as the sequence lengths n increases. The current dependence structures of record events within hydrologic sequences is a lower level than in the past, and it is a higher level than it will be in the future.

The statistics regarding the number of records within a sequence has been dealt with extensively. For a summary account refer to Arnold et al. (1998). To determine the number of record events within a region, the multivariate structure underlying the observed sequences—at least the dependence structure of the sequences—must be accounted for (see Vogel et al. 2001).

At present the literature on the statistics of records from several sequences is relatively sparse. Several definitions have been proposed for bivariate records. Arnold et al. (1998) list four definitions of bivariate records and note where others may be found in the literature. In reference to random variables X and Y , the four definitions are

1. A record of the first kind occurs at time k , if X_k exceeds all preceding X_i or Y_k exceeds all preceding Y_i , or both;
2. A record of the second kind occurs at time k , if X_k exceeds the current record value X^* or Y_k exceeds the current record value Y^* , or both;
3. A record of the third kind occurs at time k , if X_k exceeds X^* and Y_k exceeds Y^* ; and
4. A record of the fourth kind occurs at time k , if X_k exceeds all preceding X_i and Y_k exceeds all preceding Y_i .

Nagaraja et al. (2003) account for bivariate records of the second and fourth kinds assuming the underlying distribution to be the Farlie–Gumbel–Morgenstern and the normal bivariate distributions. The correlation between the number of records in each of two sequences, both of length n , and the means and standard deviations of the total number of records in the sequences are given. The hydrologic shortcoming of the Farlie–Gumbel–Morgenstern distribution, restriction to low-level dependence, is noted. Transformation of observed flood sequences at two sites on the upper Mississippi river to correspond to normally distributed marginal distributions facilitates estimation of the expected number of future record flows at the sites.

12.3 FLOOD ENVELOPE CURVES: APPLICATION OF THE THEORY OF RECORDS

We begin this section by introducing one of the most common applications of the theory of records to hydrology: envelope curves. A flood envelope curve (Figure 12-5) represents an upper bound on our flood experience in a region and is formed by the record floods for all sites in a region. This section reviews the historical (nonprobabilistic) applications of envelope curves and follows with some recent research and applications that describe how to provide a probabilistic interpretation of envelope curves. Because envelope curves provide an upper bound on our flood experience, they are

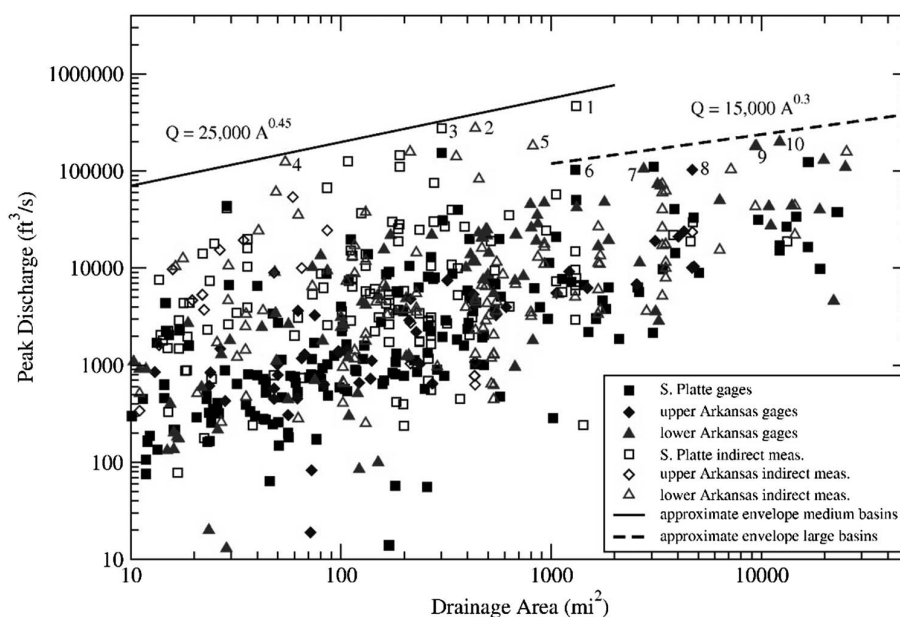


Figure 12-5. Example maximum peak discharge data, Q , and drainage area, A , envelope curve for observations within the Arkansas and South Platte River Basins in Colorado.

often compared loosely to other estimates of extraordinary floods such as the probable maximum flood. A goal of this section is to enable hydrologists to make such comparisons among extraordinary floods more objective, by including a probabilistic interpretation of all such estimates of extraordinary floods.

12.3.1 Envelope Curves: Historical Background

Envelope curves are relatively simple empirical relationships between the maximum peak flow experienced in a region and drainage area. Peak flow data are one of the most important measures of extreme floods (e.g., Dalrymple 1964). Figure 12-5 shows an example envelope curve, with the points that control the envelope summarized in Table 12-5. Figure 12-5 plots peak flow versus drainage area. Table 12-5 and Figure 12-5 show that the two flood events in June of 1921 (points 1–5) and 1965 (points 8–10) are responsible for the records that define both envelopes depicted.

The most basic envelope curve formula is that attributed to Myers (Jarvis et al. 1936, Creagher et al. 1945):

$$Q = CA^n \quad (12-42)$$

where

- Q = peak discharge (ft^3/s),
- C = coefficient,
- A = drainage area (mi^2), and
- n = exponent less than unity.

As Creagher et al. (1945, p. 125) note, values assigned to n by various investigators have ranged from 0.3 to 0.8. Based on the data for the Arkansas and South Platte Rives (Figure 12-5), a change appears to occur in the envelope curve parameters C and n that may be scale dependent.

12.3.1.1 Traditional Envelope Curve Applications

Envelope curves have a long history in flood hydrology studies (Fuller 1914, Meyer 1917, Alvord and Burdick 1918, Mead 1919, Linsley et al. 1949, Dalrymple 1964). In flood hydrology studies, regional peak discharge envelope curves are useful for four main purposes: (1) to expand the flood database for the watershed of interest with data from nearby streams, (2) to portray extreme flood potential in a region of interest, (3) to gain an understanding of the regional hydrometeorology corresponding to the largest floods on record, and (4) as a basis for comparison of probabilistic estimates of peak discharge and/or design floods. Peak flow envelope curves have traditionally been used to examine maximum floods in many locations such as the United States (Crippen and Bue 1977, O'Connor and Costa 2004), Puerto Rico (Smith et al. 2005), Italy (Marchetti 1955), and globally (Costa 1987a, Herschy 2003). They have also been used to examine physical causes of extraordinary floods on small basins (e.g., Costa 1987b) and for differentiation between rainfall and snowmelt floods (Jarrett 1990).

Flood envelope curves provide an upper bound on the maximum peak streamflow that might be expected at a site of interest based on data from the surrounding region. Usually, a record flood that lies near the envelope curve may be two or three times larger than a flood of record from a particular site within that region (Crippen and Bue 1977). Envelope curves for a region are often used as a guide to making rule-of-thumb estimates of the magnitude of high flood discharges that may be expected at a given site on a stream. For example, envelope curves have been used for comparing design flood discharges for new and existing dams (Creagher et al. 1945, Bureau of Reclamation 1987, Cudworth 1989). Envelope curves are routinely used by hydrologic and hydraulic engineers to judge the adequacy of probable maximum flood (PMF) estimates (Cudworth 1989, p. 177). They provide a useful empirical comparison of maximum observed floods within a region to the flood behavior at a particular site described by a design flood, PMF, or quantile estimate from a frequency curve. The

Table 12-5. Largest Observed Instantaneous Peak Discharge Estimates that Define the Record Flood Envelope Relation for the Arkansas and South Platte River Basins Up to Year 2005.

Point no. (fig. 12-5)	Station name	Drainage area (mi ²)	Date	Peak discharge (ft ³ /s)	Measurement type	Meas. rating	Flood type
1	Bijou Creek near Wiggins, CO	1,314.0	06/18/1965	466,000	slope-area at misc. site	poor	general storm
2	Rule Creek near Toonerville, CO	435.0	06/18/1965	276,000	slope-area at misc. site	fair	general storm
3	East Bijou Creek at Deer Trail, CO	302.0	06/17/1965	274,000	slope-area at misc. site	fair	general storm
4	Jimmy Camp Creek near Fountain, CO	54.3	06/17/1965	124,000	slope-area at misc. site	fair	general storm
5	Two Buttes Creek near Holly, CO	817.0	06/17/1965	182,000	slope-area at misc. site	good	general storm
6	South Fork Republican River near Idalia, CO	1,300.0	05/31/1935	103,000	slope-area at gauge	unknown	general storm
7	Purgatoire River at Ninemile Dam, near Higbee, CO	2,752.0	06/18/1965	105,000	estimated flow over dam at gauge	unknown	general storm
8	Arkansas River near Pueblo, CO	4,686.0	06/03/1921	103,000	slope-area at gauge	unknown	general storm
9	Arkansas River near Nepesta, CO	9,345.0	06/04/1921	180,000	slope-area at gauge	unknown	general storm
10	Arkansas River at La Junta, CO	12,29.0	06/04/1921	200,000	slope-area at gauge	unknown	general storm

largest historic peaks within a region are also used for PMF comparisons (Bullard 1986). Our probabilistic analysis of envelope curves, which is provided later on in this chapter, makes such comparisons more objective than using an envelope curve without a probabilistic basis.

Envelope curves can be used in research studies that seek to improve our understanding of the mechanisms that give rise to extraordinary floods. For example, one could explore flood seasonality, flood process (snowmelt, thunderstorms, general storms, rain on snow, etc.), and flood hydrometeorology (storm type, duration, areal extent, etc.) for each of the largest floods. This information can then be used to enhance our understanding and prediction of floods in the future. Matthai (1990) describes several limitations of envelope curves, including data quality problems, partial area rainfall/runoff representation, and the curve's nonrepresentativeness of the geologic and climatic conditions at one's point of interest.

12.3.1.2 Envelope Curve Relationships

In addition to the most commonly used envelope curve relation in Equation (12-42), several others have been proposed. Myers and Jarvis (Jarvis 1926, Jarvis et al. 1936) recommend $n = 0.5$ and use a modified form of Equation (12-42) as (see Linsley et al. 1949, p. 574):

$$Q = 100b\sqrt{A} \quad (12-43)$$

with Q and A defined as previously, and b a constant that ranges from about 1 to 300 based on data in Table 12-11 of Linsley et al. (1949). Linsley et al. (1958, p. 211) make the following remarks regarding the Myers formula [Equation (12-43)]: "Only luck will permit the selection of the correct value of b for a basin. Formulas of this type should never be used for engineering design."

Based on the data they had at the time for the United States and at other locations around the world, Creagher et al. (1945) recommend a modified form of Equation (12-42):

$$Q = 46CA^{0.894(A^{-0.048})} \quad (12-44)$$

However, they note that this envelope relation did not bound the 1940 storm in North Carolina or the May–June 1935 Texas storm. A more flexible form of an envelope curve formula with five parameters was presented by Crippen (1982):

$$Q = K_1 A^{K_2} (A^{C_1} + C_2)^{K_3} \quad (12-45)$$

where C and K are empirical constants. Meyer (1994) uses Equation (12-45) to estimate maximum flood flows in northern and central California. In addition to the aforementioned equations, many other formulas have been proposed (Jarvis et al. 1936, Creagher et al. 1945, Linsley et al. 1949).

An equivalent form of Equation (12-42) with peak flow expressed as a unit discharge q (where $q = Q/A$) is (Creagher et al. 1945)

$$q = CA^{n-1} \quad (12-46)$$

Figure 12-6 shows this common relationship, using the data from Figure 12-5. The relation in Equation (12-46) yields a straight line in log space (e.g., Jarvis 1926; Creagher et al. 1945; Matalas 1997, 2000; Castellarin et al. 2005). We recommend the use of Equation (12-46), which we employ in Section 12.3.2 for developing a probabilistic interpretation of envelope curves.

Unit discharge envelope curves can be based on other variables, such as elevation (e.g., Figure 12-7), in addition to drainage area. Castellarin et al. (2007) introduce a multivariate approach to the development of probabilistic regional envelope curves, including both geomorphologic factors and climatic factors.

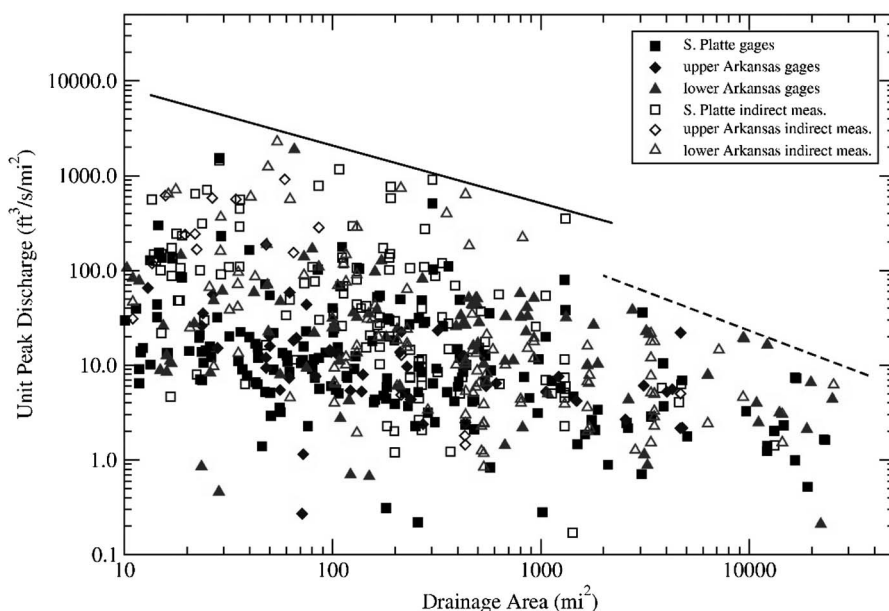


Figure 12-6. Example of maximum unit peak discharge data, q , and drainage area, A , envelope curve for observations within the Arkansas and South Platte River basins in Colorado.

Some early empirical efforts attempted to provide a probabilistic interpretation to record floods. Fuller (1914) presents three equations that relate mean annual floods, drainage area, return period, and maximum floods:

$$\bar{Q} = CA^{0.8} \quad (12-47)$$

$$Q = \bar{Q}(1 + 0.8 \log_{10} T) \quad (12-48)$$

$$Q_{max} = Q(1 + 2A^{-0.3}) \quad (12-49)$$

where

\bar{Q} = mean annual flood,

Q = greatest 24 h discharge during a period of years T (maximum 1 day flood),

Q_{max} = maximum peak flow based on the 1 day maximum, and

C = coefficient that is assumed to be constant for the river at the point of observation.

Fuller (1914) as cited in Meyer (1917) was the first to define a regional flood probability in the context of an envelope curve.

After the mid-1950s in the United States, envelope curves did not typically have any probability or frequency associated with them (Crippen and Bue 1977, Crippen 1982). As IACWD (1986, p. 71) notes, "This magnitude is unqualified by any statement of probability or frequency of occurrence. For this reason, and because the relationship between the envelope curve and the observational data is not prescribed by any specific hydrologic theory, the proper usage and interpretation of the envelope curve are not clear." For envelope curves to be most useful, a probabilistic interpretation is needed and was recently proposed by Castellarin et al. (2005) and Vogel et al. (2007).

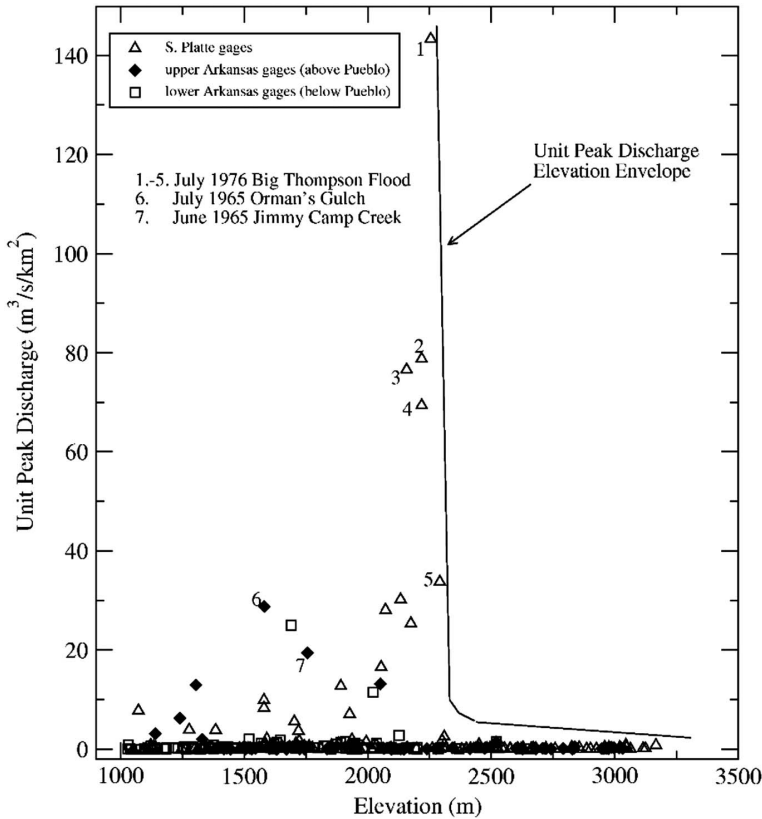


Figure 12-7. Example of flood envelope curve based on watershed elevation for observations within the Arkansas and South Platte River basins, Colorado.

Source: England et al. (2010).

12.3.2 Probabilistic Interpretation of Envelope Curves

Consider an envelope curve that plots the logarithm of the ratio of the record flood to the drainage area, $\ln(Q/A)$, versus $\ln(A)$ as was shown earlier in Figure 12-6 and Equation (12-46). We term such an envelope curve a “regional envelope curve” (REC) because it reflects our regional experience of record floods. Consider the REC in Figure 12-8 (Jarvis 1926) along with the envelope curve described by

$$\ln\left(\frac{Q}{A}\right) = a + b \ln(A) \quad (12-50)$$

If the envelope curve is assumed to be linear (in log space) with a given slope b , the intercept a in Equation (12-50) may be estimated by forcing the REC to bound all record floods to the present, say up to the year n . See Castellarin et al. (2005) as well as Equation (12-53) and (12-54) and associated discussion for further information on how to estimate the slope term b for a region. Let X_j^i denote the annual maximum flood in year $i = 1, 2, \dots, n$ at site $j = 1, 2, \dots, M$, where M is the number of sites in the region. Let $X_j^{(i)}$ denote the flood flow of rank (i) at site j , where ranking is from smallest (1) to largest (n). The REC's intercept up to the year n can then be expressed as

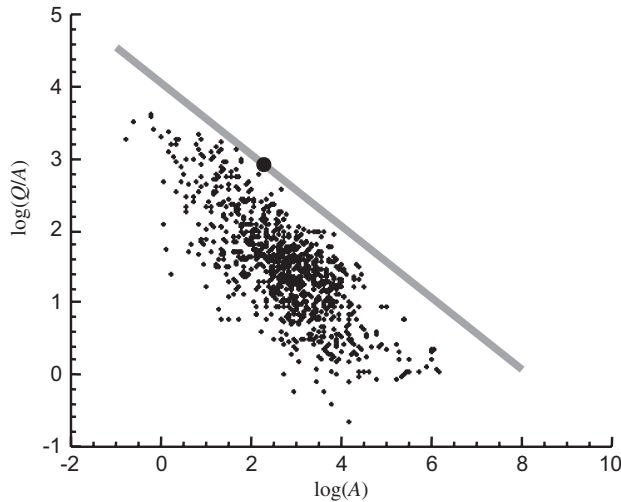


Figure 12-8. Flood experience accrued prior to 1925, discharge, Q in ft^3/s , and drainage area, A in mi^2 ; elements of experience (+) and element of experience (•) defining the intercept of the envelope curve (thick gray line).

Source: Jarvis (1926).

$$a^{(n)} = \max_{j=1, \dots, M} \left\{ \ln \left(\frac{X_j^{(n)}}{A_j} \right) - b \ln(A_j) \right\} \quad (12-51)$$

where A_j is the area of site $j = 1, 2, \dots, M$.

Castellarin et al. (2005) propose a probabilistic interpretation of an REC defined by Equation (12-50) that is based on the following assumptions:

The study region is homogeneous in the sense of the index-flood hypothesis (see, e.g., Dalrymple 1960) and therefore, the probability distribution of standardized annual maximum peak flows is the same for all sites in the region (or in the pooling group of sites; e.g., Burn 1990, Castellarin et al. 2001). The standardized annual maximum peak flow, X' , is defined for a given site as the annual maximum peak flow, X , divided by a site-dependent scale factor, μ_X (i.e., the index flood), assumed in this study to be equal to the at-site mean of X . Under this assumption, the flood quantile with exceedance probability p , denoted as x_p , is given by

$$x_p = \mu_X x'_p \quad (12-52)$$

where x'_p is the regional dimensionless flood quantile with exceedance probability p .

The relationship between the index flood μ_X and basin area A is of the form

$$\mu_X = C A^{b+1} \quad (12-53)$$

where C is a constant and b is the same as in Equations (12-50) and (12-51).

Combining Equations (12-52) and (12-53) leads to a relation between $\ln(x_p/A)$ and $\ln(A)$ that is analogous to Equation (12-50):

$$\ln \left(\frac{x_p}{A} \right) = \ln \left(\frac{\mu_X x'_p}{A} \right) = \ln(C x'_p) + b \ln(A) \quad (12-54)$$

The formal analogy between Equations (12-51) and (12-54) originates from the simplifying assumptions and implies that if the index flood scales with the drainage area, then the slope of the REC for a region can be identified from this scaling relationship. More importantly, Castellarin et al. (2005) show that the assumptions also imply that (1) a probabilistic statement can be associated with the intercept $a^{(n)}$ of Equation (12-50), which is determined from the largest standardized annual maximum peak flow observed in the region [here standardization is achieved via the index-flood method using Equation (12-53) to express the index flood], and (2) the exceedance probability (p -value) of the REC is equal to the p -value of the standardized maximum flood (hereafter referred to as regional record flood, Y').

The following two sections illustrate how, under these fundamental assumptions, the problem of estimating the exceedance probability of an REC can be placed within the context of the theory of records and the actual estimation of the exceedance probability of an REC can be addressed.

12.3.2.1 Envelope Curves and the Theory of Records

The REC provides an upper bound on record-breaking flood experiences to date and therefore is closely connected with the theory of records (Vogel et al. 2001, 2007). Castellarin et al. (2005) analyze the gains in regional flood experience summarized by the REC in the context of record-breaking events and evaluate the behavior of sequences of regional record floods for cross-correlated regions through repeated Monte Carlo simulations. See Castellarin et al. (2005) for a description of how those experiments were performed. According to the authors, the regional gain in flood experience that causes an upward shift in the REC involves all sites in the region in a “competition” to break the upper bound that forms the REC. In a region with M sites, a new record event (hereafter referred to as envelope record) occurs when *at least one site* experiences a record flood event *and* the magnitude of that flood also exceeds the upper bound identified by the current REC. When a new envelope-record event is experienced, the REC is shifted upward, with the slope b held constant, to bound the new gain in regional flood experience.

Under the hypotheses adopted here [see Equations (12-52) to (12-54)], which are identical to those described by Castellarin et al. (2005, Section 2.1), the temporal dynamics of the REC coincides with the temporal dynamics of the record-breaking process of the series of maxima of the M standardized annual floods, which is always a univariate *iid* sequence even in the presence of intersite correlation.

Figure 12-9 compares the theoretical average number of records μ_R for a univariate *iid* sequence [Equation (12-34)] with the average number of envelope records obtained from Monte Carlo

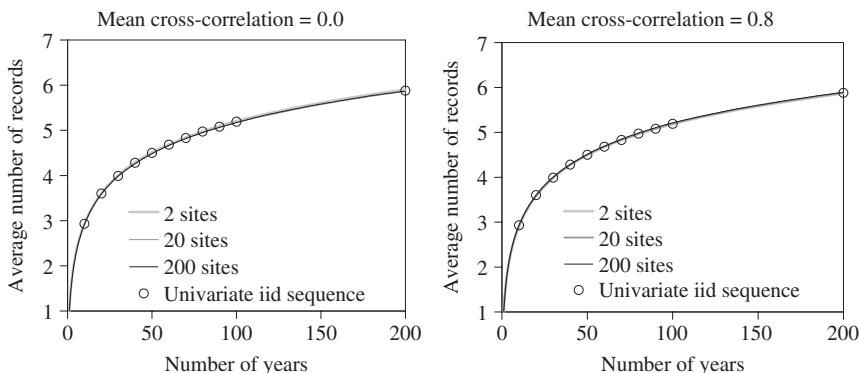


Figure 12-9. Values of μ_R for a univariate *iid* sequence of record-breaking events and average number of envelope records obtained through Monte Carlo experiments for different cross-correlated regions.

experiments. Figure 12-9 considers regions with $M = 2$ to 200 sites, each with sample lengths $n = 1$ to 200 years both with and without cross-correlation. All curves reported in Figure 12-9 are nearly coincident, and analogous outcomes can be obtained for the variance of the number of record events σ_R^2 [Equation (12-35)], showing the equivalence between the temporal dynamics of the record series for a realization of an *iid* sequence of random variables and of an REC.

Even though the moments of the number of envelope-record breaking events depend neither on the regional parent distribution of flood flows, nor on the degree of cross-correlation among flood sequences (see, e.g., Figure 12-9), these aspects are critical when estimating the exceedance probability of the envelope, as detailed in the next subsection.

12.3.2.2 Exceedance Probability of Envelope Curves

We describe how to estimate the exceedance probability of an REC under the hypotheses given in Equations (12-52) to (12-54), which are the same hypotheses as in Castellarin et al. (2005). Let the variables x_i , y_i , and z_i represent three different random variables related to the annual maximum flood at site i , the flood of record (FOR) at site i and the ordinate of the point on the envelope curve corresponding to site i , respectively. Also, let A_i denote the drainage area at site i . The scatter diagram of $\ln(y_i)$ versus $\ln(A_i)$, where $y_i \equiv x_i^{(n)}$ (FOR at site i), is an expression of our flood experience over the period $t = 1$ to $t = n$. Our experience may be bound by an enveloping line, that is, a line below which all our experience, expressed in terms of FORs and their relation to drainage area, lies (see the gray line in Figure 12-8). The enveloping line is set with a slope, b , and passes through that observation, such that all other points lie below the line, hence the name, envelope line. The envelope line [Equation (12-50)] may also be rewritten as

$$\ln(z_i) = a + b \ln(A_i) \quad (12-55)$$

Consider the derivation of the probability of exceeding the envelope curve at a particular site i at time $t = n + 1$, where, perhaps, a water project is envisaged at the site. Vogel et al. (2007) address this problem by considering a hypothetical region consisting of M sites where the sequence length n at each site is sufficiently long (in the limit as $n \rightarrow \infty$), such that the matrix of the correlations between record values may be represented by an identity matrix, $\mathbf{W} \approx \mathbf{I}$ [see Equations (12-39) and (12-40)]. At time $t = n + 1$, the flood at site i will be a flood of record, R_i at that site with probability

$$P(R_i) = (n + 1)^{-1}; \forall i \quad (12-56)$$

Given that the flood of record event R_i occurs at site i , the record flood will exceed the envelope value at that site, E_i with probability given by

$$P(E_i | R_i) = \int_{z_i}^{\infty} dG_{(n)}(Y_i) \quad (12-57)$$

where z_i denotes the ordinate of the point on the envelope line given in Equation (12-55) corresponding to the abscissa, $\ln(A_i)$, whereas

$$G_{(n)}[Y_i] = F^n[X_i] = \Pr[Y_i > y_i] \quad (12-58)$$

is the distribution of the FOR in a sequence of length n .

Of interest here is the occurrence of both events E_i and R_i , at time $t = n + 1$, that is, having observed at time $t = n + 1$ a record flood at site i that also exceeded the envelope. This particular event, which we term $E_i R_i$, will occur with exceedance probability given by

$$\begin{aligned} P(E_i R_i) &= P(R_i) P(E_i | R_i) \\ &= (n + 1)^{-1} \int_{z_i}^{\infty} dG_{(n)}(Y_i) \end{aligned} \quad (12-59)$$

Note that all sites are not equal because site $i = i'$ is the site that defines the current ($t = n$) envelope and for which the record flood, $z_{i'} = x_{i'}^{(n)}$, falls on the envelope curve. All future record floods at that site will exceed the envelope line, so that

$$P(E_{i'} | R_{i'}) = \int_{z_i = x_{i'}^{(n)}}^{\infty} dG_{(n)}(y_{i'}) = 1 \quad (12-60)$$

whereby

$$\begin{aligned} P(E_{i'} R_{i'}) &= P(R_{i'}) P(E_{i'} | R_{i'}) \\ &= P(R_{i'}) \\ &= (n + 1)^{-1} \end{aligned} \quad (12-61)$$

If a water project is contemplated at site i , then of particular interest at that site is the local exceedance probability in year $(n + 1)$ of the envelope line defined in year n , that is, the probability that the flow in year $(n + 1)$ at site i will exceed the envelope line defined in year n (see [Vogel et al. 2007](#)):

$$\begin{aligned} \Phi_i(z_i) &= \begin{cases} P(E_{i'} R_{i'}); & \text{if } i = i' \\ P(E_i R_i); & \text{if } i \neq i' \end{cases} \\ &= \begin{cases} (1 + n)^{-1}; & \text{if } i = i' \\ (1 + n)^{-1} \int_{z_i}^{\infty} dG_{(n)}(Y_i); & \text{if } i \neq i' \end{cases} \end{aligned} \quad (12-62)$$

Equation (12-62) yields an exceedance probability corresponding to the ordinate of the point on the envelope line z_i corresponding to the abscissa, $\ln(A_i)$, based on M samples, each of length n . Hence the probability $\Phi_i(z_i)$ is a random variable with a distribution and moments that depend upon the distributional properties of both the ordinate of the envelope line z_i as well as the flood series at site i .

[Vogel et al. \(2007\)](#) consider two summary measures of $\Phi_i(z_i)$: (1) its expectation $E[\Phi_i(z_i)]$, which we term the expected exceedance probability of an envelope (*EEPE*), and (2) $\Phi_i(E[z_i])$, which we term the exceedance probability of the expected envelope (*EPEE*). The *EEPE* is defined by

$$E[\Phi_i(z_i)] = \begin{cases} (1 + n)^{-1}; & \text{if } i = i' \\ \int_0^{\infty} \left[(1 + n)^{-1} \int_{z_i}^{\infty} G_{(n)}(Y_i) dz \right] g_{(Mn)}(z_i) dz; & \text{if } i \neq i' \end{cases} \quad (12-63)$$

where $g_{(Mn)}(z_i) = \frac{dG_{(Mn)}(z_i)}{dz}$ and $\Phi_i(z_i)$ is given in Equation (12-62). Here $g_{(Mn)}(z_i)$ represents the pdf associated with the value of the envelope curve at a particular site i . Because the envelope is defined by flood series at M independent sites, each of length n , the record length associated with the pdf of z , $g_{(Mn)}(z_i)$, is equal to Mn . Similarly, the *EPEE* is defined by

$$\Phi_i(E[z_i]) = \begin{cases} (1+n)^{-1}; & \text{if } i = i' \\ (1+n)^{-1} \int_{\mu_z}^{\infty} dG_{(n)}(Y_i); & \text{if } i \neq i' \end{cases} \quad (12-64)$$

where μ_z denotes the expectation of z .

The summary measures *EPEE* and *EEPE* represent two different probabilistic statements regarding an envelope curve. If one's concern is with making a probabilistic statement regarding the single envelope based on historical observations, then *EEPE* is an appropriate summary measure, whereas if one's concern is with making a probabilistic statement regarding the expected envelope, then *EPEE* is an appropriate summary measure.

For example, if flood series x arises from a GUM model with cumulative distribution function given in Equation (12-4), and the envelope curve is based on Mn iid GUM observations, according to Equation (12-7a) the expectation of the envelope curve is given by

$$\mu_z = \xi + \alpha(\gamma + \ln(Mn)) \quad (12-65)$$

where ξ is the GUM location parameter, α is the GUM scale parameter, M is the number of sites, each with sample size n , and γ is the Euler number.

Substitution of Equation (12-65) into Equation (12-64) yields the cdf of the record flood at site i denoted as $G_{(n)}(Y_i)$, whereby the exceedance probability of the envelope given in Equation (12-64) becomes

$$\Phi_i(z_i) = \frac{1 - G_{(n)}(z_i)}{n+1} = \frac{1 - \exp\left(-n \exp\left(-\frac{z_i - \xi}{\alpha}\right)\right)}{n+1}; \quad \text{for } i \neq i' \quad (12-66)$$

The *EPEE* is obtained by substitution of $z_i = \mu_z$ from Equation (12-65) into Equation (12-66), which, after subsequent algebra, leads to

$$\Phi_i(\mu_z) = EPEE = \frac{1 - \exp\left(-\frac{\exp(-\gamma)}{M}\right)}{n+1}; \quad \text{for } i \neq i' \quad (12-67)$$

where $\Phi_i(\mu_z)$ denotes the exceedance probability associated with the expected envelope curve μ_z , at site i , when flows are iid as Gumbel.

The *EEPE* for the GUM case is obtained by substitution of $\Phi_i(z_i)$, given by Equation (12-66), and $g_{(mn)}(z_i) = \frac{dG_{(mn)}(z_i)}{dz}$ into Equation (12-63), which leads to

$$\begin{aligned} E[\Phi_i(z_i)] &= EEPE = \int_0^{\infty} \frac{1 - \exp\left(-n \cdot \exp\left(-\frac{z - \xi}{\alpha}\right)\right)}{n+1} \frac{dG_{(mn)}(z_i)}{dz} dz \quad \text{for } i \neq i' \\ &= \frac{1}{n+1} \left[1 - \frac{M}{M+1} \left(1 - \exp\left(-n(M+1) \cdot \exp\left(\frac{\pi}{C_v \sqrt{6}} - \gamma\right)\right) \right) \right] \\ &\approx \frac{1}{(n+1)(M+1)} \end{aligned} \quad (12-68)$$

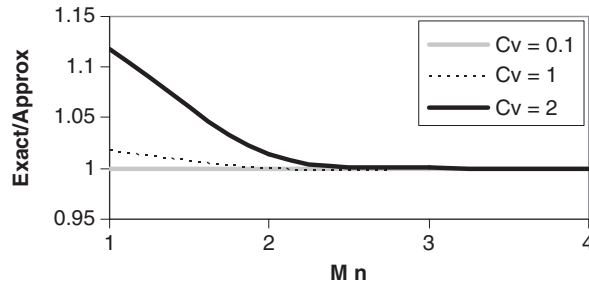


Figure 12-10. Comparison of the exact and approximate expressions for EEPE given in Equation (12-68).

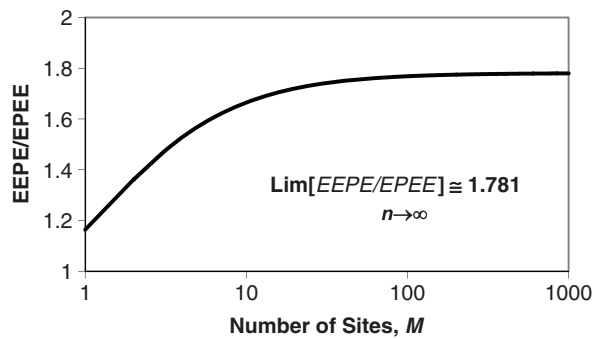


Figure 12-11. Comparison of the ratio of EEPE (Equation (12-68)) to EPEE [Equation (12-67)] for the Gumbel case (M = no. of sites and n = sample size at each site).

where C_v is the coefficient of variation of the annual maximum flood flows x . Figure 12-10 illustrates the ratio of the exact and approximate expressions for EEPE given in Equation (12-68) as a function of M , n , and C_v . Figure 12-10 (see also Vogel et al. 2007) illustrates that the approximation is generally excellent whenever the product $Mn > 3$, regardless of the value of C_v .

Figure 12-11 (Vogel et al. 2007) provides a comparison of the values of EPEE and EEPE for the Gumbel case and illustrates that the values of EEPE are always greater than those of EPEE. Figure 12-11 illustrates that over the range of values of M considered, the increase in the ratio of EEPE to EPEE as M increases strongly indicates that the ratio converges to a value equal to approximately 1.781. Vogel et al. (2007) prove the correctness of the analytic expressions of EPEE and EEPE for the iid GUM case through a series of Monte Carlo simulation experiments and provide a close analytical expression of the EPEE for the iid GEV case, which using the usual notation reads

$$\Phi_i(\mu_z) = EPEE = \frac{1 - \exp\left[-\frac{(\Gamma(1+\kappa))^{1/\kappa}}{M}\right]}{n+1}; \quad \text{if } i \neq i' \quad (12-69)$$

where $\Gamma(\cdot)$ is the gamma function and κ is the shape parameter of the GEV distribution. As expected, EPEE for the GEV case in Equation (12-69) reduces to EPEE for the GUM case in Equation (12-67) as κ approaches zero.

12.3.3 Exceedance Probability of Empirical Envelope Curves

In most practical applications, the datasets that can be used to construct empirical envelope curves consist of a limited number of years (i.e., the hypothesis that in the limit $n \rightarrow \infty$ cannot be applied).

In addition, actual flood records in neighboring watersheds often exhibit significant values of the cross-correlation coefficient. Nonetheless, it is exactly under these circumstances that an estimation of the exceedance probability of the envelope curve is needed for the design and operation of large dams. Recall that if one's concern is with making a probabilistic statement regarding the single envelope curve based on historical observations, then *EEPE* is an appropriate summary measure, whereas if one's concern is with making a probabilistic statement regarding the expected envelope curve, then *EPEE* is an appropriate summary measure. This subsection illustrates how to estimate *EPEE* for envelope curves constructed from real-world datasets that exhibit limited flow records of varying length and are cross-correlated. We are unaware of any efforts as of yet to estimate *EEPE* from such real-world datasets.

Castellarin et al. (2005) show under two fundamental hypotheses (see beginning of Section 12.3.2) the problem of estimating the *EPEE* reduces to estimating the exceedance probability of the largest value in a regional sample of standardized annual maximum peak flows (i.e., observed peak flows divided by the mean annual flood). Their work's primary challenge involves estimation of the regional information content of concurrent cross-correlated flood series of equal length. Castellarin et al. (2005) use results from Matalas and Langbein (1962) and Stedinger (1983) to quantify the regional information content using the concept of the equivalent number of independent annual maxima. Castellarin et al. (2005) express the equivalent number of independent observations, or number of effective observations n_{eff} , as n times the equivalent number of independent sequences M_{EC} , which can be estimated from

$$\hat{M}_{EC} = \frac{M}{1 + \overline{\rho^\beta}(M-1)}, \text{ with } \beta = 1.4 \frac{(nM)^{0.176}}{(1-\rho)^{0.376}} \quad (12-70)$$

where $\overline{\rho^\beta}$ and $\overline{(1-\rho)^{0.376}}$ are average values of the corresponding functions of the correlation coefficients [i.e., $\overline{\rho^\beta}$ is the average of the $M(M-1)/2$ values of $\rho_{k,j}^\beta$, where $\rho_{k,j}$ is the correlation coefficient between annual maximum floods at sites k and j , with $1 \leq k < j \leq M$]. Although here we assume that $\rho_{k,j}$ is the linear correlation between the annual maximum floods, one could also define it as the linear correlation between the logarithms of the annual maximum floods (see, e.g., Stedinger 1981). Castellarin (2007) presents an algorithm that relaxes the need for concurrent series, enabling the estimation of n_{eff} for real-world datasets.

For a regional dataset consisting of M annual maximum series (AMS) that span n years, the actual distribution of the flood series in time (e.g., missing data, different installation years for different gauges, etc.) can be taken into account as follows. First, one identifies the number of years, n_1 , for which the original dataset includes only one observation of the annual maximum discharge, that is $M-1$ observations are missing (for example, some gauges may not be operational, or may not be installed yet). These n_1 observations are effective by definition. Second, the dataset containing the $n - n_1$ remaining years is subdivided into $N_{sub} \leq (n - n_1)$ subsets; each one of them (say subset s) is selected in such a way that all its $L_s \leq M$ sequences are concurrent and of equal length l_s and are therefore suitable for the application of the estimator proposed by Castellarin et al. (2005). Using this splitting criterion, the effective number of observations n_{eff} can be calculated as the summation of the effective sample years of data estimated for all N_{sub} subsets,

$$\hat{n}_{eff} = n_1 + \sum_{s=1}^{N_{sub}} \hat{n}_{eff,s} = n_1 + \sum_{s=1}^{N_{sub}} \frac{L_s l_s}{1 + \left[\overline{\rho^\beta} \right]_{L_s} (L_s - 1)}, \text{ with } \beta = 1.4 \frac{(L_s l_s)^{0.176}}{\left[(1-\rho)^{0.376} \right]_{L_s}} \quad (12-71)$$

For a description of the development of Equation (12-72), see Castellarin et al. (2005, Equation 19).

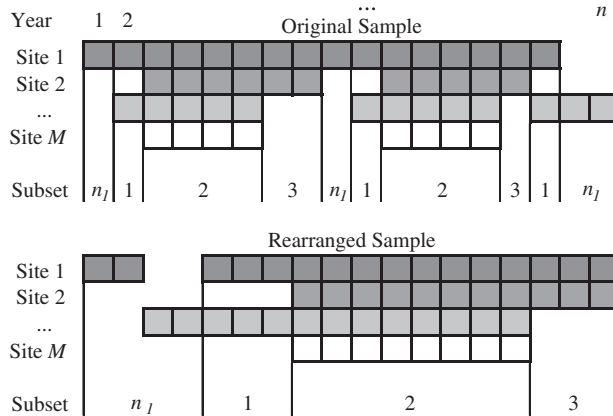


Figure 12-12. Subdivision of a descriptive example of M annual maximum series of flood flows that globally span n years (each square represents one observation) into n_l single observations and three subsets (i.e., 1, 2, and 3) containing only concurrent sequences of equal length. The rearranged sample highlights the subdivision.

As described previously, n_l represents the number of times annual floods were observed at one site only (and possibly single observations or indirect measurements at miscellaneous sites), that is, the total number of years in which $L_s = 1$. The notation $[\cdot]^{L_s}$ in Equation (12-71) indicates that the average terms ρ^β and $(1 - \rho)^{0.376}$, which have the same meaning as in Equation (12-70), are to be computed with respect to the $L_s > 1$ annual flood sequences that form subset s . The β exponent in Equation (12-70) coincides formally with β in Equation (12-71). This is consistent with the fact that the L_s sequences forming each subset s are concurrent and of equal length (l_s) (e.g., see Figure 12-12), which was the condition adopted for the identification of the empirical relationship in Equation (12-71).

The $EPEE$ value can be estimated by representing the intersite correlation from a suitable model of cross-correlation versus distance between sites (see, e.g., Tasker and Stedinger 1989, Troutman and Karlinger 2003) and by using an appropriate plotting position with the overall sample years of data set equal to \hat{n}_{eff} . Castellarin (2007) shows that the selection of the cross-correlation model has limited impact on the reliability of $EPEE$ values and recommends the use of the model introduced by Tasker and Stedinger (1989) to approximate the true annual peak cross-correlation function $\rho_{i,j}$ as a function of the distance $d_{i,j}$ among sites i and j ,

$$\rho_{i,j} = \exp\left(-\frac{\lambda_1 d_{i,j}}{1 + \lambda_2 d_{i,j}}\right) \quad (12-72)$$

where $\lambda_1 > 0$ and $\lambda_2 \geq 0$ are the regional parameters that may be estimated by either ordinary or weighted least squares procedures.

Castellarin (2007) addresses the problem of selecting a suitable plotting position for estimating $EPEE$. Cunneane (1978) introduces the general plotting position:

$$\hat{p}_{EE} = 1 - \frac{\hat{n}_{eff} - \eta}{\hat{n}_{eff} + 1 - 2\eta} \quad (12-73)$$

where η is the plotting position parameter, and \hat{n}_{eff} is the empirical estimate of n_{eff} given in Equation (12-71). Each plotting position is characterized by a particular η value (see, e.g., Table 12-6

Table 12-6. Parameterization of a Probabilistic Regional Envelope Curve (p).

Name	Description*	η	T_{EC}
Weibull	Probability unbiased for all distributions	0.00	$n_{eff} + 1$
Cunnane	Approximately quantile unbiased	0.40	$1.67 \cdot n_{eff} + 0.3$
Gringorten	Optimized for Gumbel distribution	0.44	$1.79 \cdot n_{eff} + 0.2$
Hazen	A traditional choice	0.50	$2 \cdot n_{eff}$
GEV	Quantile unbiased for the maximum of a GEV sample	$0.44 - 0.46 \cdot \kappa$	$\frac{n_{eff} + 0.12 + 0.92\kappa}{0.56 + 0.46\kappa}$

*See also Stedinger et al. (1993).

Note: Plotting positions: η is the parameter of the plotting position as in Equation (12-75); κ is the shape parameter of the GEV distribution; n_{eff} is the effective sample years of data; and $T_{EC} = 1/EPEE$ is the recurrence interval assigned to n_{eff} .

for selection criteria). The results reported in Castellarin (2007) indicate that, among several possible options, a quantile-unbiased plotting position should be used for estimating EPEE. Castellarin (2007) derives a quantile-unbiased plotting position for use with the GEV distribution. The proposed plotting position is a very compact and easy to apply asymptotic formula for the estimation of the exceedance probability of the largest value in a GEV sample, in which the parameter η of Equation (12-73) depends on the shape parameter κ of the fitted GEV distribution,

$$\eta(k) = \frac{\exp(\gamma) - 1}{\exp(\gamma)} - \frac{\pi^2}{12 \exp(\gamma)} \kappa; \quad \eta(\kappa) = 0.44 - 0.46 \kappa \quad (12-74)$$

where, as usual, $\gamma = 0.5772$ is Euler's constant. Equation (12-74) should only be applied when $n_{eff} \geq 10$ and $-0.5 < \kappa < 0.5$.

12.4 APPLICATIONS OF THE THEORY OF RECORDS: CASE STUDIES

The following sections provide three case studies. The first two case studies derive probabilistic regional envelope curves based on (1) annual maximum flood observations in north central Italy and (2) precipitation observations in Austria. The third case study examines the record-breaking properties of flood observations for the continental United States.

12.4.1 Application of Probabilistic Regional Envelope Curves

This section summarizes two real-world applications of the theory of records. In both cases, an estimate of the average recurrence interval $T_{EC} = EPEE$ associated with the expected regional envelope curve is obtained. The first example assesses the applicability of probabilistic regional envelopes of flood flows for design-flood estimation in ungauged basins over a wide geographical region in north central Italy (see Castellarin 2007). The second example refers to the construction of probabilistic envelope curves for record rainfall events of various durations that were observed in Tyrol (Austria). The second example also provides an assessment of the resulting probabilistic envelope curve using a very long synthetic rainfall series generated through a stochastic rainfall model (Viglione et al. 2012). Other practical applications of probabilistic regional envelopes of record floods may be found in Guse et al. (2009, 2010) for the region of Saxony, Germany, and in Padi et al. (2011) for the African continent, while probabilistic envelopes of extreme rainstorms are also developed in Castellarin et al. (2009) for north central Italy.

12.4.1.1 Probabilistic Regional Envelope Curves for Flood Flows in North Central Italy

We briefly summarize an application of probabilistic regional envelope curves performed by [Castellarin \(2007\)](#). The study considers flood discharge data for 33 unregulated catchments in north central Italy, which are illustrated in Figure 12-13. The discharge data were collected by the National Hydrographic and Hydrometric National Service of Italy. The record length at the stations varies from a minimum of 15 years to a maximum of 74 years with a mean value of 32 years.

Previous studies indicate that the flood frequency regime presents only a limited degree of heterogeneity over the whole study area and proposes a subdivision of the area into three subregions with an acceptable degree of homogeneity. Also, the GEV distribution was shown to be a suitable regional parent distribution for the annual maximum flood flow sequences in the study area ([Castellarin 2007](#) and references therein).

Figure 12-13 reports three subregions (regions W, western; C, central; and E, eastern), which mainly reflect climatic differences existing in the study area. Table 12-7 lists some characteristics of the study area, such as the number of sites, the overall sample years of data, the number of years for

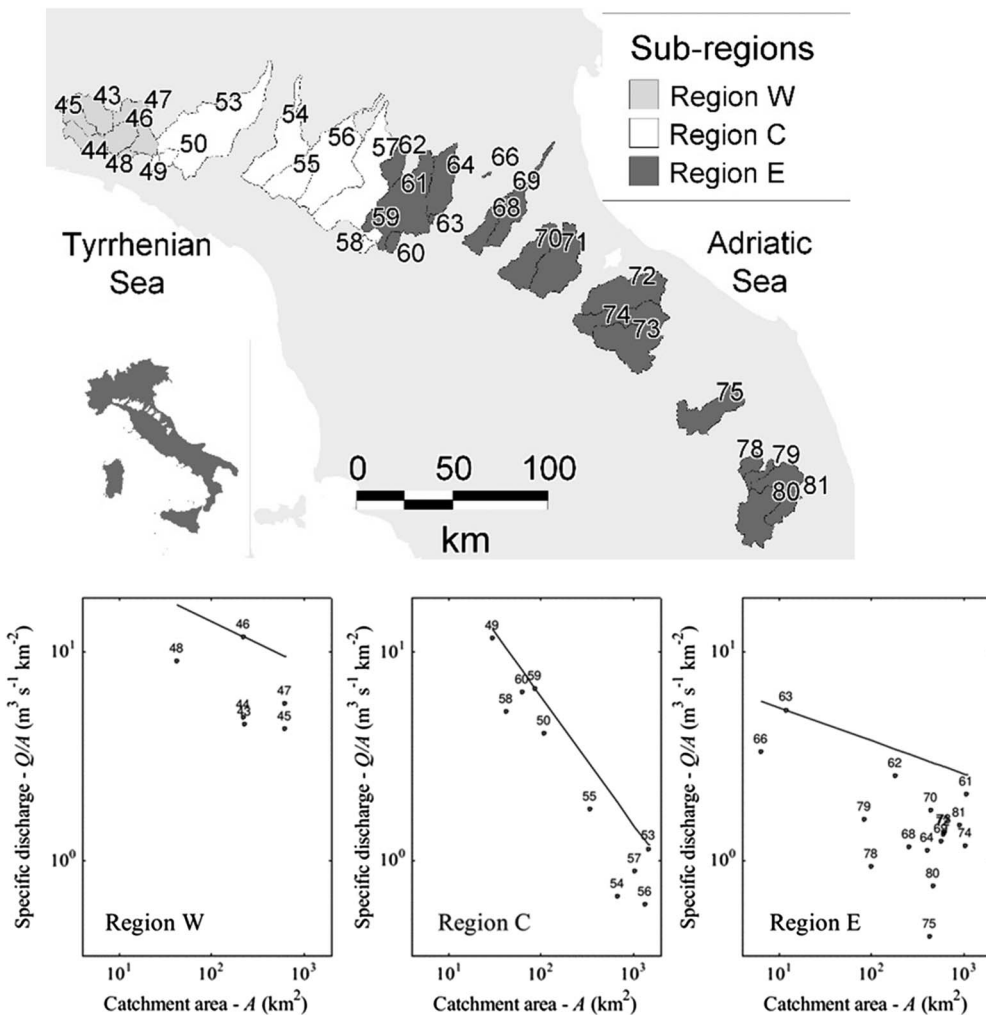


Figure 12-13. North central Italy: 33 basins, grouped into three homogeneous regions (top panel), and empirical regional envelope curves for the three subregions of the study area (bottom panel).

Table 12-7. Characteristics of Regions W, C, and E in N Italy.

Characteristics	Region W	Region C	Region E
Number of sites	6	10	17
Number of observations	159	339	572
Number of single observations (n_1)	12	0	11
Estimated shape parameter κ	-0.34	-0.09	-0.11
Estimated envelope slope [see Equation (12-55)], \hat{b}	-0.21	-0.61	-0.16
Calculated envelope intercept [see Equation (12-55)], a	3.61	4.62	2.05
Parameter λ_1 (km^{-1}) of the correlation model (see Equation 12-72)	For all 3 regions: $4.052 \cdot 10^{-5}$		
Parameter λ_2 (km^{-1}) of the correlation model (see Equation 12-72)	For all 3 regions: $1.606 \cdot 10^{-5}$		
Parameter of the GEV plotting position, $\eta(k)$ of (see Equation 12-74)	0.596	0.481	0.490
Recurrence interval, T_{EC} (years)	258	412	751

which annual floods are available at one site only [i.e., n_1 in Equation (12-71)], and a regional estimate of the shape parameter κ of the GEV estimated as described in Hosking and Wallis (1997).

Figure 12-13 illustrates envelope curves constructed for regions W, C, and E. Table 12-7 reports the estimates of the parameters λ_1 and λ_2 of the cross-correlation model in Equation (12-72) obtained for the entire study area. The estimates were obtained by applying a weighted least squares regression algorithm that weights each sample cross-correlation coefficient between two sequences (sites) proportionally to the number of concurrent annual floods. Table 12-7 also reports the estimates of the envelope slopes \hat{b} , obtained by regressing the empirical values of the index-flood (i.e., at-site estimates of mean annual flood) against the drainage areas of the corresponding basins, along with the values of the intercept a , computed as follows,

$$a = \max_{j=1, \dots, M} \left\{ \ln \left(\frac{Q_j}{A_j} \right) - \hat{b} \ln(A_j) \right\} \quad (12-75)$$

where Q_j denotes the maximum flood observed at site $j = 1, 2, \dots, M$, and M is the number of sites in the region, while A_j is the area of site j . Recall that Equation (12-75) is based on the index flood assumption as was discussed earlier in Section 12.3.2. Finally, Table 12-7 lists the coefficients η of the plotting position estimator calculated using the asymptotic relation of Equation (12-74) as a function of the κ values, and the resulting estimate of the expected recurrence interval, $T_{EC} = 1/EPEE$. Recall that T_{EC} is the expected recurrence interval associated with our estimate of the effective record length n_{eff} associated with the expected envelope. The probabilistic envelope curves in Figure 12-13 can be used to obtain a graphical estimate of the T_{EC} year flood (envelope flood quantile) at any ungauged site within each region as a function of the catchment area alone (T_{EC} values are indicated in Table 12-7).

Castellari (2007) assesses the reliability of estimates of envelope flood quantiles for ungauged sites through a comprehensive cross-validation procedure. Those experiments illustrate that the accuracy of envelope quantiles are comparable to the reliability of regional predictions produced by the application of the index-flood approach. In summary, envelope flood quantiles are attractive because they (1) can be easily determined for ungauged sites graphically as a function of the catchment area alone, (2) do not require any extrapolation of an assumed flood frequency distribution, and (3) were shown to be conservative by Castellari (2007) in that overestimation tends to prevail due to the possible presence of regional heterogeneities.

9.4.1.2 Probabilistic Regional Envelope Curves for Record Rainfall Events in Tyrol, Austria

Castellarin et al. (2009) first introduced depth–duration envelope curves (DDECs), which, analogous to RECs for flood flows, are graphical representations of the maximum observed point rainfall depth (or record rainfall depth) for a given duration over a region. Of interest here is the probabilistic interpretation of DDECs which Castellarin et al. (2009) introduces, which is analogous to the probabilistic interpretation of RECs for flood flows. The probabilistic interpretation of DDECs relies on the assumption that the spatial variability of rainfall annual maxima for a given duration τ can be described by the variability of mean annual precipitation (MAP). Viglione et al. (2012) show that if (1) the L-moment ratios of rainfall extremes can be assumed to be constant in space and (2) a nondecreasing scaling law holds between the mean annual maximum rainfall depth m_τ (for duration τ) and MAP, an analytical relationship results between the local MAP value and the T year rainfall depth quantile associated with duration τ , $h_{\tau,T}$. When L-moment ratios can be assumed to be constant in space and the scaling law between m_τ and MAP assumes the form

$$m_\tau = a_\tau \cdot \text{MAP}^{b_\tau} \quad (12-76)$$

the relationship between $h_{\tau,T}$ and MAP becomes

$$\frac{h_{\tau,T}}{\text{MAP}} = k_{\tau,T} \cdot \frac{m_\tau}{\text{MAP}} = k_{\tau,T} \cdot a_\tau \cdot \text{MAP}^{(b_\tau-1)} \quad (12-77)$$

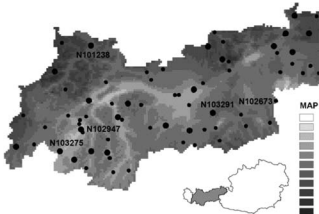
where a_τ and b_τ are regional coefficients, whereas $k_{\tau,T}$ is a growth factor depending on duration τ and recurrence interval T . Probabilistic DDECs were applied and validated in north central Italy (Castellarin et al. 2009) and in the Austrian district Tyrol (Viglione et al. 2012). A brief illustration of the Austrian application is reported here below.

Tyrol is located in the western part of Austria within the Alpine region and has an area of about 10,600 km². Table 12-8 describes the study area and the available raingauge network.

An envelope of the record rainstorms observed in the study area for the durations of interest can be fit using a mathematical relationship analogous to Equation (12-77), in which $k_{\tau,T}$ is replaced by a coefficient, which we term $k_{\tau,\text{MAX}}$, whose meaning is analogous to the intercept a in Equation (12-75) for the REC of flood flows and that can be computed from the observed rainfall data as

$$k_{\tau,\text{MAX}} = \max_{j=1,\dots,M} \left\{ \frac{h_{\tau,\text{MAX},j}}{\hat{a}_\tau \cdot \text{MAP}_j^{b_\tau}} \right\} \quad (12-78)$$

Table 12-8. The 73 Rain Gauges in Tyrol (Austria) Considered in Viglione et al. (2012), the 22 Stations Used for the Comparison are Highlighted in Black; the Gray Scale Shows the Mean Annual Precipitation (MAP).

	No. of gauges	73		
	Altitude (m a.s.l.)	493 (min)	1,297 (mean)	2,850 (max)
	MAP (mm)	548 (min)	1,110 (mean)	1,732 (max)
	Series length (years)	1 (min)	10 (mean)	31 (max)
	Station-years of data	695		

Note: a.s.l. = above sea level.

Table 12-9. Characteristics of the Annual Maximum Rainfall Depths for Different Durations, Calibrated Coefficients of the Cross-Correlation Formula [Equation (12-72)], Empirical DDEC Parameters, and Estimated Recurrence Interval (the Number of Stations Considered Is 73 for a Total of 695 Observations for All Durations).

Duration τ (hours):	0.25	1	3	6
Estimate of b_τ in Equation (12-77)	0.682	0.518	0.440	0.433
Estimate of a_τ in Equation (12-77)	0.091	0.490	1.15	1.59
Calculated $k_{\tau, \text{MAX}}$ in Equation (12-78)	3.80	3.51	3.49	2.94
Parameter λ_1 (10^{-4} km^{-1}) of the correlation model, Equation (12-72)	5.99	8.87	4.57	5.40
Parameter λ_2 (10^{-4} km^{-1}) of the correlation model, Equation (12-72)	2.05	2.84	1.41	3.38
Number of effective observations \hat{n}_{eff} in Equation (12-71)	663.9	679.5	665.0	484.1
Recurrence interval, T (years)	1,328	1,359	1,330	968

where estimates of a_τ and b_τ of Equation (12-78) are obtained through a regression analysis; $h_{\tau, \text{MAX}, j}$ in Equation (12-78) denotes the maximum rainfall depth observed for duration τ at site $j = 1, 2, \dots, M$, and M is the number of sites in the region; and MAP_j is the local value of the mean annual precipitation.

RECs for flood flows and DDECs for rainfall are analogous concepts that share an identical probabilistic interpretation. An estimated recurrence interval can be associated with $k_{\tau, \text{MAX}}$. The empirical estimator of the number of effective observations [Equation (12-71)] yields an estimate of the exceedance probability of the empirical DDECs. Table 12-9 reports the estimates of the parameters of the model [Equation (12-77)] for the durations of interest, together with the estimates of the number of effective observations and the corresponding estimated recurrence intervals obtained by applying a suitable plotting position.

Viglione et al. (2012) assess the validity of the recurrence intervals estimated for each empirical DDEC by comparing the envelope curves with quantiles of rainfall depth associated with the same recurrence intervals retrieved from very long series of synthetic rainfall series generated through an adaptation of the stochastic rainfall model presented in Sivapalan et al. (2005). Viglione et al.'s (2012) stochastic rainfall model was calibrated locally (i.e., site by site) for a subset of 22 gauges spanning the entire range of empirical MAP values (see Figure 12-14) and evenly scattered over the study region (see Table 12-8). Figure 12-15 illustrates the results of this comparison, showing a good agreement between DDECs and rainfall quantiles retrieved from long synthetic series, thus supporting the meaningfulness of the proposed DDECs and the reliability of their probabilistic interpretation. For further details, the interested reader is referred to Viglione et al. (2012).

12.4.2 Record-Breaking Properties of Floods in the United States

The theory of records offers a framework for understanding the probabilistic behavior of extreme events, which is nearly independent of the theory of extremes. Thus examining probabilistic properties of floods is possible without resorting to assumptions regarding a probability distribution. Other than a probability distribution, the other common assumption is that floods are *iid* events. Because the *iid* assumption is the only assumption required for most theoretical results pertaining to record events, the theory of records has been suggested for testing the *iid* assumption (Foster and Stuart 1954). This is a very unique aspect of the theory of records, that is, many of the theoretical results only depend on the single *iid* assumption. Thus an evaluation of whether or not samples behave as expected under the theory of records may be considered a test of the *iid* assumption. In the

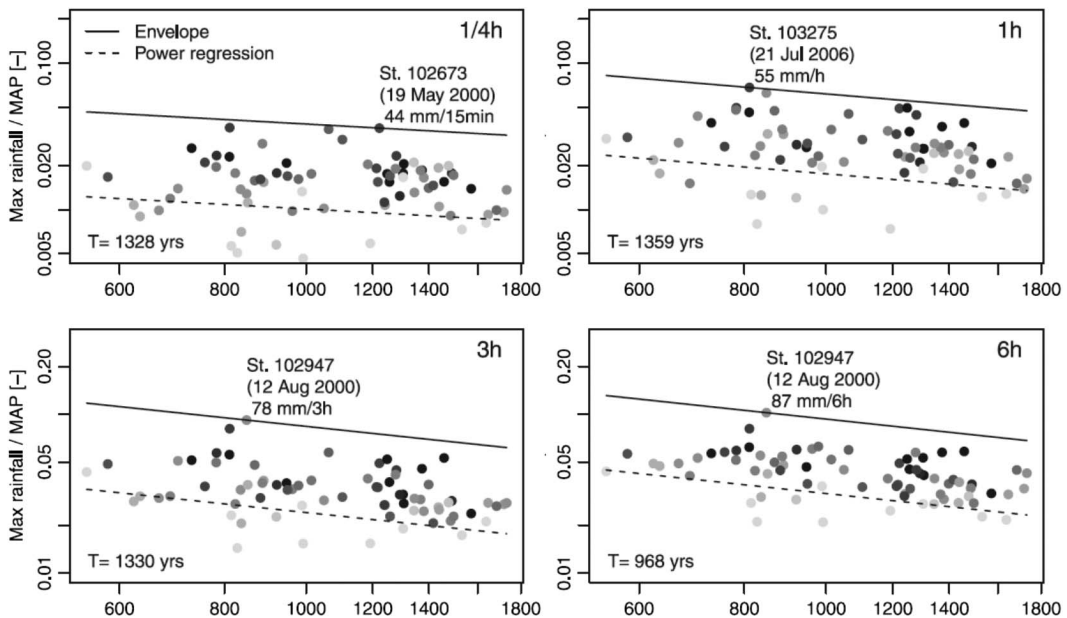


Figure 12-14. DDECs for different durations (0.5 to 6 h) in Tyrol, Austria. The circles represent MAP versus the rescaled maximum recorded rainfall depth for the 73 rainfall stations. The grayscale is proportional to the sample lengths. The envelope curve of Equation (12-77) is shown by the continuous line. The dashed line represents the scaling relation between (m_r/MAP) and MAP of Equation (12-76).

following example from Vogel et al. (2001), the record-breaking properties of historical annual maximum flood records in the United States were examined to determine whether or not they behave like serially independent events.

To perform these experiments, the Hydro-Climatic Data Network (HCDN) compiled by Slack et al. (1993) was employed, which comprises average streamflow values recorded on a daily, monthly, and annual basis in the entire United States spanning the time period 1874–1988. For the purpose of this study, only data pertaining to the 48 conterminous states were considered, which correspond to 18 water resources regions. To enable an effective summary of our results, three meta-regions of the United States were employed: the east, midwest, and west. Respectively, these consist of two-digit HUs 1–6, 7–12, and 13–18. This analysis does not consider regions outside of the continental, conterminous United States of America.

Observations of floods in a region are correlated in space, which influences the sampling properties of the moments of the number of record events, R , given in Equations (12-34 to 12-37). The record-breaking properties were derived for serially independent but spatially correlated events, as in Section 12.2.3. To detect any serial dependence of the record-breaking floods in the United States, the record-breaking frequency of actual floods was compared with their theoretical counterparts.

In Figures 12-16 to 12-18, theoretical and sample estimates of the mean, standard deviation, and coefficient of variation of the number of record floods in an n year period were compared for the eastern, midwestern, and western regions of the United States, respectively. Sample estimates of skewness and kurtosis are known to be significantly biased, so they were not calculated (Wallis et al. 1974, Vogel and Fennessey 1993). The vertical lines (with the small horizontal lines at the end) on either side of the theoretical values denote approximate 89% Chebyshev 3σ error bars for each statistic (Ross 1994). Chebyshev's inequality for any random variable X with mean μ and variance σ^2 is given by

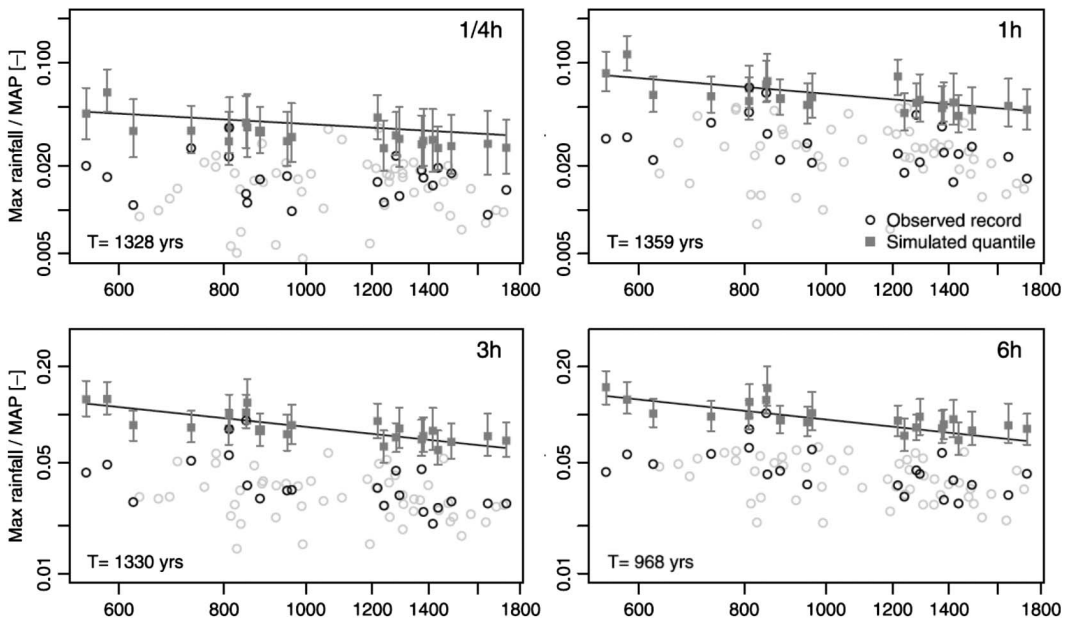


Figure 12-15. Comparison between empirical DDECs and synthetic rainfall quantiles for the return period given by the DDEC procedure. The figure is analogous to Figure 12-14 but only the 22 stations used for the comparison are highlighted (open black circles). The rainfall quantiles, resulting from the stochastic generation of 1 million years of rainfall, are indicated by solid gray squares. The 90% confidence bounds are also indicated in gray.

$$P[|X - \mu| \geq c] \leq \frac{\sigma^2}{c^2} \quad (12-79)$$

where c is a constant equal to half the width of the confidence interval; which here is set equal to 3σ , which implies that $P[|X - \mu| \geq 3\sigma] \leq 0.11$, or else $P[|X - \mu| \leq 3\sigma] \geq 0.89$, which is a crude approximation, but very convenient here as it can be easily parameterized to document the influence of spatial correlation on the width of the derived intervals. Analogous confidence intervals are constructed for the statistics s_R and $C_v[R]$. The heavy confidence intervals denote intervals based on the assumption of spatial independence ($\rho = 0$) of the flood observations. The light-weight confidence intervals (shown only for μ_R) are based on the assumption that the cross-correlation of the flood observations is equal to the average cross-correlation of flow records for all sites in the region. According to Walker (1999), average cross-correlations of the annual maximum flow records in the eastern, midwestern, and western regions of the United States are 0.23, 0.19, and 0.42, respectively. These sample estimates of the average spatial correlation of the annual maximum flood series were computed for all possible pairs of observations, which had at least 10 years of record in common. Employing the regional average value of cross-correlation is the simplest approach to describe the distribution of spatial correlations in a region.

Stedinger (1983), Hosking and Wallis (1988), and Douglas et al. (2000) also use regional average values of cross-correlation to describe the dependence between flow series at different sites. Douglas et al. (2000) compare the use of regional trend tests of US flood records based on (1) regional average spatial cross-correlations and (2) the boot-strap approach for preserving the empirical regional distribution of the spatial dependence of flood observations. They find good agreement between these two approaches. Nevertheless, our use of a regional average spatial cross-correlation is a gross simplification, because the complex spatial and temporal climatic mechanisms, which give rise to

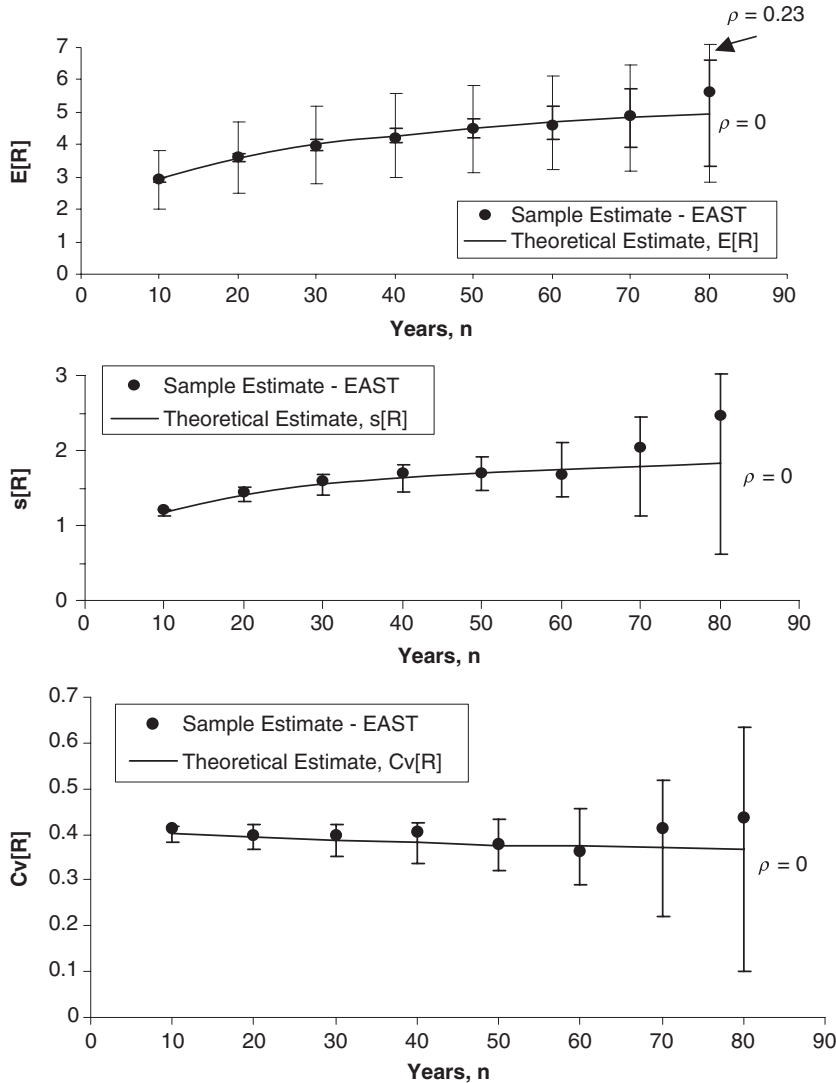


Figure 12-16. Comparison of the sample and theoretical estimates of $E[R]$, $s[R]$, and $C_v[R]$ as a function of n for the eastern region.

flood observations, will lead to spatial correlation structures, which in turn depend strongly upon how the regions are defined.

In computing the moments of the number of record events, R , all possible overlapping sets of n year periods within the HCDN database were considered. Table 12-10 reports the number of such nonoverlapping n year periods available in each region. The reason that confidence intervals widen as n increases is due to the fact that in each region the number of nonoverlapping sets of n year samples decreases as n increases. The confidence intervals reflect the increasing uncertainty associated with our ability to determine properties of record-breaking events as n increases. If smaller regions were used, the confidence intervals would have widened. If the sample estimates of mean R , reported in top graph of Figures 12-16 to 12-18, fall within the reported 89% confidence intervals for μ_R (which account for cross-correlation), it can be concluded that the flood series in that region are serially independent, because that was the only assumption required for the theoretical

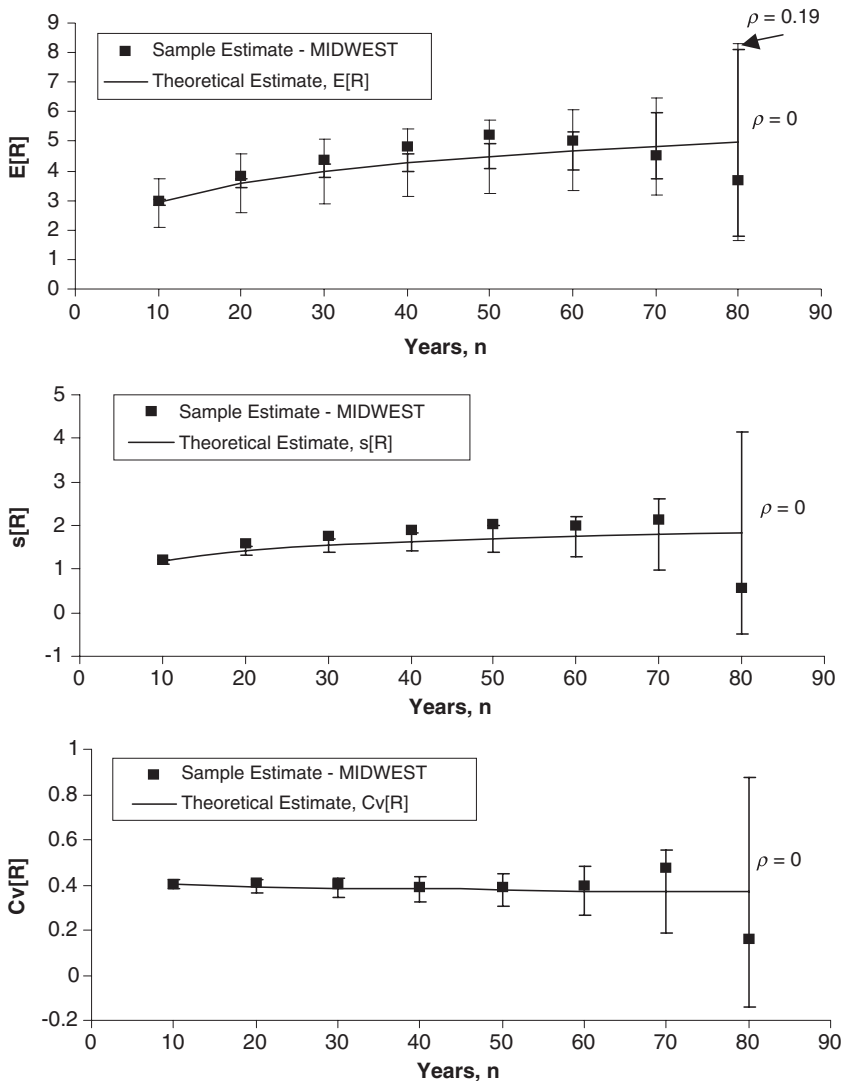


Figure 12-17. Comparison of the sample and theoretical estimates of $E[R]$, $s[R]$, and $C_v[R]$ as a function of n for the midwestern region.

analysis. Note that the confidence intervals for μ_R , which account for the spatial correlation of the flood observations, are much wider than the confidence intervals that assume spatial independence.

In general, Figures 12-16 to 12-18 illustrate that when one accounts for the spatial correlation of the flood observations, the observed regional mean R falls within the 89% confidence intervals for μ_R for all three US regions. However, if the flood observations are assumed to be spatially independent (which they are not), we would mistakenly conclude that flood observations in the midwestern and western regions of the United States are serially dependent. Hence our results indicate that flood observations in the eastern United States are consistent with the theory of record-breaking phenomena for serially independent processes. This example shows that the theory of record-breaking processes provides a comprehensive mathematical framework for evaluating the frequency and magnitude of extreme events and can be applied to identifying nonstationarity in hydrological records.

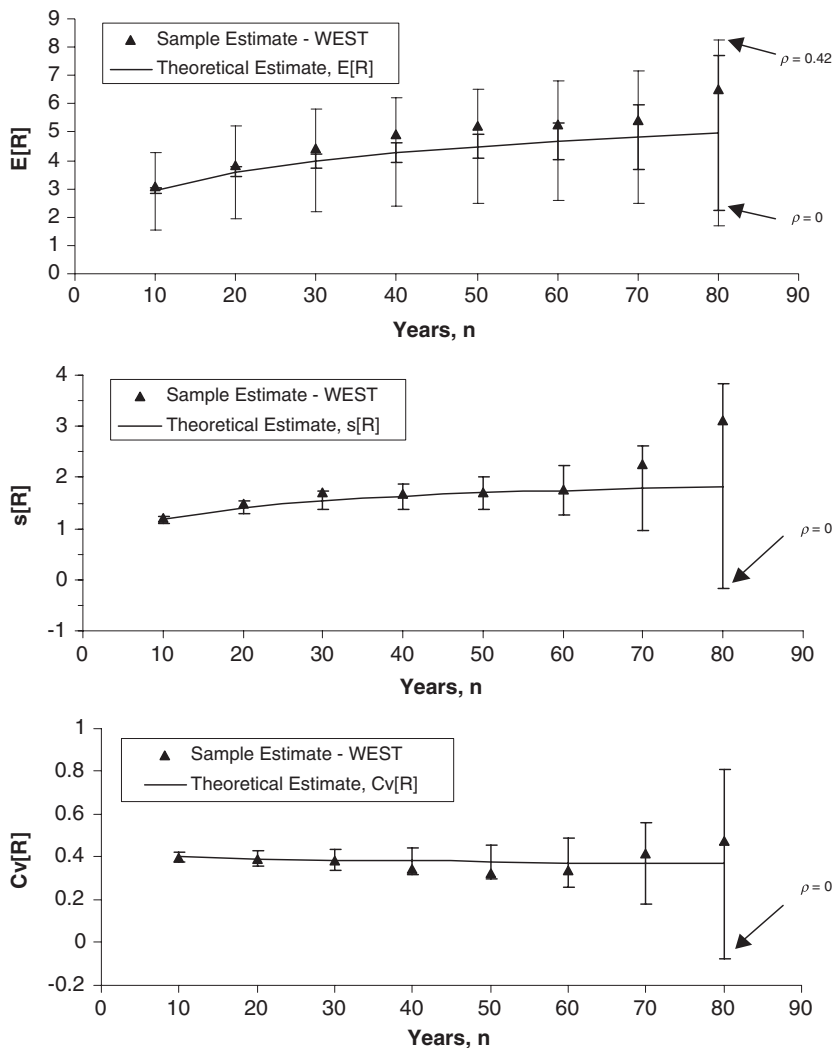


Figure 12-18. Comparison of the sample and theoretical estimates of $E[R]$, $s[R]$, and $C_v[R]$ as a function of n for the western region.

Table 12-10. Number of Nonoverlapping n -Year Periods in Each Region.

Record Length, n	East	Midwest	West
10	2,680	1,919	1,561
20	1,164	838	665
30	650	432	350
40	418	278	200
50	270	151	136
60	112	66	63
70	36	23	22
80	11	3	4
Total	5,341	3,710	3,001

12.5 CONCLUSIONS

We have reviewed various theoretical properties associated with the record-breaking behavior of a single time series or many sets of such observations. While our focus has been on flood and extreme rainfall events, the theory described here applies to many other natural hazards, including droughts, landslides, earthquakes, wind loads, sea levels, temperatures and others. We have discussed parametric record-breaking properties, which generally depend on assumptions concerning the probability distribution of the observations. We have also discussed nonparametric record-breaking properties, which generally only depend on the assumption that the series is independent and identically distributed.

The theory of records relies heavily upon the theory of order statistics (David and Nagaraja 2003) and extreme order statistics, as well as on the theory of extremes (Gumbel 1958). Interestingly, much of the theory of records is independent of the theory of extremes. Remarkably, only recently was the theory of records first applied to water resources data (Vogel et al. 2001), thus many opportunities exist for new avenues of research concerning record processes. We have summarized two recent case studies, which have applied the theory of records to assign an exceedance probability associated with an envelope curve of extreme hydrological events (i.e., floods and rainstorms)—a task that was thought to be impossible before Vogel et al.'s (2007) work. We have also summarized a case study that explored the nonparametric record-breaking properties of flood events in the continental United States. Given ever-increasing concerns over the degree of change associated with the future frequency and magnitude of natural hazards, developments and applications associated with the theory of records are likely to play an increasingly important role.

Because a fundamental assumption associated with much of the theory of records involves an assumption of stationarity, extensions to the theory may be needed to account for nonstationary record processes. For example, many examples now extend the stationary theory of extremes into the nonstationary domain (e.g., Furrer et al. 2010, Sankarasubramanian and Lall 2003, Towler et al. 2010, Vogel et al. 2011; Serago and Vogel, 2018; Salas et al. 2018). Similar extensions are needed to enable the theory of records to account for nonstationary processes.

As it has been emphasized, an attractive property of the theory of records is that much of the theory only depends upon the assumption that flood sequences are *iid*. Two properties under the *iid* assumption in the theory of records complicate the task of determining the extent to which observed sequences yield record events that accord with the theory. First, the expected number of records reflected by a sequence of length n is very sparse. For “long” hydrologic sequences, $n \sim 100$, the expected number of record events is about 5. For long surrogate hydrologic sequences (e.g., tree rings and mud varves, $n \sim 1,000$), the expected number of record events is about 7.5. For sequences of geologic length, $n \sim 1,000,000$, the expected number of record events is about 14.4. The longer a sequence is, the more pronounced is the degree of sparsity of record events. Second, regardless of the length of a sequence, record events tend to occur early in the sequence. The longer the sequence is, the more apparent is the “earliness.” As put by Arnold et al. (1998), “we shall never see the 50th record-breaking event, for in expectation, we will all be dead”. These two factors and others render the task of detecting evidence counter to the *iid* assumption quite challenging.

Many fundamental hydrologic problems depend critically upon an understanding of the theory of extremes, records, and order statistics. We expect that combining these three theories, along with developments in nonstationarity and Bayesian statistics, may lead to numerous extensions to the results presented here. For example, the traditional concepts of the probable maximum precipitation (PMP) and the probable maximum flood (PMF) are used widely in the design of hydraulic structures, yet have never been fully analyzed within the domain of the theory of record processes. Only recently has a rigorous theoretical approach to a probabilistic assessment of the PMP (Koutsoyiannis 1999, Salas et al. 2013) and PMF (Vogel et al. 2007, Salas et al. 2013) been given.

Tremendous opportunities remain associated with the application of the theory of records to estimation of extreme rainfall and flood probabilities, including traditional deterministic criteria, such as the PMP and PMF.

References

- Ahsanullah, M. 1995. *Record statistics*, 227. Hauppauge, NY: Nova Science Publishers.
- Ahsanullah, M. 2004. *Record values—Theory and applications*, 314. Dallas: University Press of America.
- Alvord, J. W., and C. B. Burdick. 1918. *Relief from floods*, 175. New York: McGraw-Hill.
- Ang, A. H-S., and W. H. Tang. 1984. *Probability concepts in engineering planning and design: Volume II Decision, risk and reliability*. New York: Wiley.
- Arnold, B. C., N. Balakrishnan, and H. N. Nagaraja. 1998. *Records*, 312. New York: Wiley.
- Arnold, B. C., N. Balakrishnan, and H. N. Nagaraja. 2008. "Record values." Vol. 54 in *First course in order statistics, classics in applied mathematics*, 241–257. Philadelphia, PA: SIAM.
- Balakrishnan, N., and M. Ahsanullah. 1994. "Recurrence relations for single and product moments of record values from generalized Pareto distribution." *Commun. Stat.-Theor. Methods* 23 (10): 2841–2852.
- Bardossy, A., and S. Horning. 2016. "Gaussian and non-Gaussian inverse modeling of groundwater flow using copulas and random mixing." *Water Resour. Res.* 52 (6): 4504–4526.
- Beirlant, J., Y. Goegebeur, J. Segers, and J. Teugels. 2004. *Statistics of extremes*, 490. Hoboken, NJ: Wiley.
- Bullard, K. L. 1986. *Comparison of estimated probable maximum flood peaks with historic floods*, 165. Denver: Bureau of Reclamation, Hydrology Branch.
- Bureau of Reclamation. 1987. *Design of small dams*. 3rd ed., 860. Denver: US Dept. of Interior, Bureau of Reclamation.
- Burn, D. H. 1990. "Evaluation of regional flood frequency analysis with a region of influence approach." *Water Resour. Res.* 26 (10): 2257–2265.
- Butkiewicz, J., and E. Hys. 1977. "On a Class of Bi- and Multivariate Distributions Generated by Marginal Weibull Distributions." In Vol. 7A *Transaction of the 7th Prague Conf on Information Theory, Statistical Decision Functions, Random Processes and of the 1974 European Meeting of Statisticians*, edited by J. Koźechnik. Dordrecht, The Netherlands: Springer.
- Castellarin, A. 2007. "Application of probabilistic envelope curves for design-flood estimation at ungaged sites." *Water Resour. Res.* 43 (4): W04406.
- Castellarin, A., D. H. Burn, and A. Brath. 2001. "Assessing the effectiveness of hydrological similarity measures for regional flood frequency analysis." *J. Hydrol.* 241 (3–4): 270–285.
- Castellarin, A., R. Merz, and G. Blöschl. 2009. "Probabilistic envelope curves for extreme rainfall events." *J. Hydrol.* 378 (3–4): 263–271.
- Castellarin, A., R. M. Vogel, and N. C. Matalas. 2005. "Probabilistic behavior of a regional envelope curve." *Water Resour. Res.* 41 (6): W06018.
- Castellarin, A., R. M. Vogel, and N. C. Matalas. 2007. "Multivariate probabilistic regional envelopes of extreme floods." *J. Hydrol.* 336 (3–4): 376–390.
- Chandler, K. N. 1952. "The distribution and frequency of record values." *J. R. Stat. Soc. Ser. B.* 14 (2): 220–228.
- Chowdhury, J. U., J. R. Stedinger, and L.-H. Lu. 1991. "Goodness-of-fit tests for regional generalized extreme value flood distributions." *Water Resour. Res.* 27 (7): 1765–1776.
- Costa, J. E. 1987a. "A comparison of the largest rainfall-runoff floods in the United States with those of the People's Republic of China and the world." *J. Hydrol.* 96 (1–4): 101–115.
- Costa, J. E. 1987b. "Hydraulics and basin morphology of the largest flash floods in the conterminous United States." *J. Hydrol.* 93 (3): 313–338.
- Creagher, W. P., J. D. Justin, and J. Hinds. 1945. *Engineering for dams. Vol. I. General design*, 99–140. New York: Wiley.
- Crippen, J. R. 1982. "Envelope curves for extreme flood events." *J. Hydraul. Eng.* 108 (HY10): 1208–1212.
- Crippen, J. R., and C. D. Bue. 1977. *Maximum flood flows in the conterminous United States: US Geological Survey Water-Supply Paper 1887*. Washington, DC: US Printing Office.
- Cudworth, A. G. Jr. 1989. *Flood hydrology manual*, 243. Denver: US Dept. of Interior, Bureau of Reclamation.
- Cunnane, C. 1978. "Unbiased plotting positions—A review." *J. Hydrol.* 37 (3–4): 205–222.
- Dalrymple, T. 1960. *Flood frequency analyses: US Geological Survey Water Supply Paper 1543-A*. Reston, VA: USGS.

- Dalrymple, T. 1964. "Hydrology of flood control. Part I: Flood characteristics and flow determination." In *Handbook of hydrology*, edited by V. T. Chow. New York: McGraw-Hill.
- David, F. N., and D. E. Barton. 1962. *Combinatorial chance*. New York: Hafner, 178–183.
- David, H. A., and H. N. Nagaraja. 2003. *Order statistics*. 3rd ed. New York: Wiley.
- Douglas, E. M., and R. M. Vogel. 2006. "The probabilistic behavior of floods of record in the United States." *J. Hydrol. Eng.* **11** (5): 482–488.
- Douglas, E. M., R. M. Vogel, and C. N. Kroll. 2000. "Trends in floods and low flows in the United States: Impact of spatial correlation." *J. Hydrol.* **240** (1–2): 90–105.
- England, J. F., Jr., J. E. Godaire, R. E. Klinger, and T. R. Bauer. 2010. "Paleohydrologic bounds and extreme flood frequency of the Arkansas River Basin, Colorado, USA." *Geomorphology* **124** (1–2): 1–16.
- Enzel, Y., L. L. Ely, P. K. House, V. R. Baker, and R. H. Webb. 1993. "Paleoflood evidence for a natural upper bound to the flood magnitudes in the Colorado River basin." *Water Resour. Res.* **29** (7): 2287–2297.
- Fisher, R. A., and L. H. C. Tippett. 1928. "Limiting forms of the frequency distributions of the largest and smallest members of a sample." In *Mathematical Proc., Cambridge Philosophical Society*.
- Foster, F. G., and A. Stuart. 1954. "Distribution-free tests in time-series based on the breaking of records, with discussion." *J. R. Stat. Soc. Ser. B.* **16**: 1–22.
- Fuller, W. E. 1914. "Flood flows." *Trans. Am. Soc. Civ. Eng.* **1293** (77): 564–617. 618–694.
- Furrer, E. M., R. W. Katz, M. D. Walter, and R. Furrer. 2010. "Statistical modeling of hot spells and heat waves." *Clim. Res.* **43** (3): 191–205.
- Glick, N. 1978. "Breaking records and breaking boards." *Am. Math. Mon.* **85** (1): 2–26.
- Gumbel, E. J. 1958. *Statistics of extremes*, 375. New York: Columbia University Press.
- Gumbel, E. J. 1961. "The return period of order statistics." *Ann. Inst. Stat. Math.* **12** (3): 249–256.
- Guse, B., A. Castellarin, A. H. Thielen, and B. Merz. 2009. "Effects of intersite dependence of nested catchment structures on probabilistic regional envelope curves." *Hydrol. Earth Syst. Sci.* **13** (9): 1699–1712.
- Guse, B., A. H. Thielen, A. Castellarin, and B. Merz. 2010. "Deriving probabilistic regional envelope curves with two pooling methods." *J. Hydrol.* **380** (1–2): 14–26.
- Hershchy, R. 2003. *World catalogue of maximum observed floods: IAHS-AISH Publication No. 284*. Oxfordshire, UK: International Association of Hydrological Sciences.
- Hosking, J. R. M., and J. R. Wallis. 1988. "The effect of intersite dependence on regional flood frequency-analysis." *Water Resour. Res.* **24** (4): 588–600.
- Hosking, J. R. M., and J. R. Wallis. 1997. *Regional frequency analysis: An approach based on L-moments*. Cambridge, MA: Cambridge University Press.
- Husler, J., and R.-D. Reiss. 1989. "Maxima of normal random vectors: Between independence and complete dependence." *Stat. Probab. Lett.* **7** (4): 283–286.
- IACWD (Interagency Advisory Committee on Water Data). 1986. *Feasibility of assigning a probability to the probable maximum flood*. Washington, DC: US Interagency Advisory Committee on Water Data, Hydrology Subcommittee.
- Jarrett, R. D. 1990. "Paleohydrologic techniques used to define the spatial occurrence of floods." *Geomorphology* **3** (2): 181–195.
- Jarvis, C. S. 1926. "Flood flow characteristics." *Trans. Am. Soc. Civ. Eng.* **89** (1): 985–1032.
- Jarvis, C. S., et al. 1936. *Floods in the United States, magnitude and frequency*. US Geological Survey Water-Supply Paper 771. Reston, VA: USGS.
- Jenkinson, A. F. 1955. "The frequency distribution of the annual maximum (or minimum) values of meteorological elements." *Q. J. R. Meteorol. Soc.* **81** (348): 158–171.
- Kallache, M., P. Naveau, and M. Vrac. 2013. "Spatial assessment of precipitation deficits in the Duero basin (central Spain) with multivariate extreme value statistics." *Water Resour. Res.* **49** (10): 6716–6730.
- Katz, R. W., M. B. Parlange, and P. Naveau. 2002. "Statistics of extremes in hydrology." *Adv. Water Resour.* **25** (8–12): 1287–1304.
- Koutsoyiannis, D. 1999. "A probabilistic view of Hershfield's method for estimating probable maximum precipitation." *Water Resour. Res.* **35** (4): 1313–1322.
- Lambert, J. H., and D. Li. 1994. "Evaluating risk of extreme events for univariate-loss functions." *J. Water Resour. Plann. Manage.* **120** (3): 382–399.
- Linsley, R. K., M. A. Kohler, and J. L. H. Paulhus. 1949. *Applied hydrology*, 689. New York: McGraw-Hill.
- Linsley, R. K., M. A. Kohler, and J. L. H. Paulhus. 1958. *Hydrology for engineers*, 340. New York: McGraw-Hill.

- Marchetti, G. 1955. "Sulle massime portate di piena osservate nei corsi d'acqua italiani a tutto il 1953." [In Italian.] *Giorn. Genio* **104** (93): 3–4.
- Matalas, N. C. 1997. "Stochastic hydrology in the context of climate change." *Clim. Change* **37** (1): 89–101.
- Matalas, N. C. 2000. *Note on the envelope curve*. Vienna, VA.
- Matalas, N. C., and W. B. Langbein. 1962. "Information content of the mean." *J. Geophys. Res.* **67** (9): 3441–3448.
- Matthai, H. F. 1990. "Floods." In *Surface water hydrology*, edited by M. G. Wolman and H. C. Riggs. Boulder, CO: Geological Society of America.
- Mead, D. W. 1919. *Hydrology, the fundamental basis of hydraulic engineering*. New York: McGraw-Hill, 647.
- Meyer, A. F. 1917. *Elements of hydrology*, 487. New York: Wiley.
- Meyer, R. W. 1994. *Potential hazards from floodflows within the John Muir House National Historic Site, Franklin Creek drainage basin, California*. US Geological Survey Water-Resources Investigations Rep. No. 93-4009. Reston, VA: USGS.
- Nagaraja, H. N., P. K. Choudhary, and N. C. Matalas. 2003. "Number of records in a bivariate sample with application to Missouri River flood data." *Methodol. Comput. Appl. Probab.* **4** (4): 377–391.
- Nevzorov, V. B. 2001. *Records: Mathematical theory*. Providence, RI: American Mathematical Society, 164.
- O'Connor, J. E., and J. E. Costa. 2004. "Spatial distribution of the largest rainfall-runoff floods from basins between 2.6 and 26, 000 km² in the United States and Puerto Rico." *Water Resour. Res.* **40**: W01107.
- Padi, P. T., G. Di Baldassarre, and A. Castellarin. 2011. "Floodplain management in Africa: Large scale analysis of flood data." *Phys. Chem. Earth* **36** (7–8): 292–298.
- Raqab, M. Z. 2004. "Generalized exponential distribution: Moments of order statistics." *Stat. J. Theor. Appl. Stat.* **38** (1): 29–41.
- Roberts, W. C. 1991. "Human records and a tribute to the Guinness Book of World Records." *Am. J. Cardiol.* **68** (2): 288–289.
- Ross, S. 1994. *A first course in probability*. Englewood Cliffs, NJ: Prentice-Hall.
- Salas, J. D., G. Gavalan, F. R. Salas, P. Julien, and J. Abdullah. 2013. "Uncertainty of the PMP and PMF." Vol. 2 of *Handbook of engineering hydrology: Modeling, climate changes and variability*. Boca Raton, FL: CRC Press.
- Salas, J. D., J. Obeysekera, and R. M. Vogel. 2018. "Techniques for assessing water infrastructure for nonstationary extreme events: A review." *Hydrol. Sci. J.* **63** (3): 325–352.
- Salvadori, G., F. Durante, C. De Michele, M. Bernardi, and L. Petrella. 2016. "A multivariate copula-based framework for dealing with hazard scenarios and failure probabilities." *Water Resour. Res.* **52** (5): 3701–3721.
- Sankarasubramanian, A., and U. Lall. 2003. "Flood quantiles in a changing climate: Seasonal forecasts and causal relations." *Water Resour. Res.* **39** (5): 1134.
- Schucany, W. R., W. C. Parr, and J. E. Boyer. 1978. "Correlation structure in Farlie-Gumbel-Morgenstern distributions." *Biometrika* **65** (3): 650–653.
- Serago, J., and R. M. Vogel. 2018. "Parsimonious nonstationary flood frequency analysis." *Adv. Water Resour.* **112**: 1–16.
- Serinaldi, F. Kilsby. 2018. "Unsurprising surprises: The frequency of record-breaking and overthreshold hydrological extremes under spatial and temporal dependence." *Water Resour. Res.* **54** (9): 6460–6487.
- Sibuya, M. 1960. "Bivariate extreme statistics." *Ann. Inst. Stat. Math.* **11** (3): 195–210.
- Sivapalan, M., G. Blöschl, R. Merz, and D. Gutknecht. 2005. "Linking flood frequency to long-term water balance: Incorporating effects of seasonality." *Water Resour. Res.* **41** (6): W06012.
- Slack, J. R., A. M. Lumb, and J. M. Landwehr. 1993. *Hydro-climatic data network (HCDN): Streamflow data set 1874–1988*. Water Resource Investigations Rep. No. 93-4076. Reston, VA: USGS.
- Smith, J. A., P. Sturdevant-Rees, M. L. Baek, and M. C. Larsen. 2005. "Tropical cyclones and the flood hydrology of Puerto Rico." *Water Resour. Res.* **41** (6): W06020.
- Stedinger, J. R. 1981. "Estimating correlations in multivariate streamflow models." *Water Resour. Res.* **17** (1): 200–208.
- Stedinger, J. R. 1983. "Estimating a regional flood frequency distribution." *Water Resour. Res.* **19** (2): 503–510.
- Stedinger, J. R., R. M. Vogel, and E. Foufoula-Georgiou. 1993. "Frequency analysis of extreme events." In *Handbook of hydrology*, edited by D. R. Maidment. New York: McGraw-Hill.
- Tasker, G. D., and J. R. Stedinger. 1989. "An operational GLS model for hydrologic regression." *J. Hydrol.* **111** (1–4): 361–375.

- Towler, E., B. Rajagopalan, E. Gilleland, R. S. Summers, D. Yates, and R. W. Katz. 2010. "Modeling hydrologic and water quality extremes in a changing climate: A statistical approach based on extreme value theory." *Water Resour. Res.* **46** (11): W11504.
- Troutman, B. M., and M. R. Karlinger. 2003. "Regional flood probabilities." *Water Resour. Res.* **39** (4): 1095.
- Viglione, A., A. Castellarin, M. Rogger, R. Merz, and G. Blöschl. 2012. "Extreme rainstorms: Comparing regional envelope curves to stochastically generated events." *Water Resour. Res.* **48** (1): W01509.
- Vogel, R. M., and N. Fennessey. 1993. "L moment diagrams should replace product moment diagrams." *Water Resour. Res.* **29** (6): 1745–1752.
- Vogel, R. M., N. C. Matalas, J. F. England Jr., and A. Castellarin. 2007. "An assessment of exceedance probabilities of envelope curves." *Water Resour. Res.* **43** (7): W07403.
- Vogel, R. M., and I. Wilson. 1996. "The probability distribution of annual maximum, minimum and average streamflow in the United States." *J. Hydrol. Eng.* **1** (2): 69–76.
- Vogel, R. M., C. Yaindl, and M. Walter. 2011. "Nonstationarity: Flood magnification and recurrence reduction factors in the United States." *J. Am. Water Resour. Assoc.* **47** (3): 464–474.
- Vogel, R. M., A. Zafirakou-Koulouris, and N. C. Matalas. 2001. "Frequency of record breaking floods." *Water Resour. Res.* **37** (6): 1723–1731.
- Von Mises, R. 1936. "La distribution de la grande de n valeurs." [In French.] *Rev. Math. Union Interbalcanique* **1**: 141–160. Reproduced in Selected papers of Richard von Mises, II, 1964. Providence, RI: American Mathematical Society, 271–294.
- Walker, F. R. Jr. 1999. "Long term variability in flood arrival rates: The presence of annual flood event clustering." Ph.D. dissertation, Cornell Univ.
- Wallis, J. R., N. C. Matalas, and J. R. Slack. 1974. "Just a moment!." *Water Resour. Res.* **10** (2): 211–219.
- Wilks, S. S. 1959. "Recurrence of extreme observations." *J. Aust. Math. Soc.* **1** (1): 106–112.
- Zafirakou-Koulouris, A. 2000. "Statistical methods for floods and droughts." Ph.D. dissertation, Tufts Univ.

Index

- advective limit for ET, 75–76, 75*e*
- analytical probabilistic stormwater models (APSWM): conversion from exceedance probability to return period, 351–352; derived probability distribution theory, 342–343; flood control analysis, 354–360, 355*t*, 356*f*–358*f*, 359*t*; overview, 336–338; rainfall characterization, 338–340; rainfall event characteristics, 339–340, 339*t*; rainfall-runoff transformation, 340–341; runoff event peak discharge rate, 343–345; runoff event volume, 343; runoff routing through channel reaches, 348–351; runoff routing through detention ponds, 345–348, 346*f*
- annual extremes for different durations, 24*t*–25*t*, 24–26, 26*f*, 50–51, 69*f*–70*f*
- APSWM. *see* analytical probabilistic stormwater models
- aquifers. *see* groundwater hydrology
- Archimedean copulas, 420–421, 422*f*, 422*t*
- ARMA modeling: low flow analysis, 290–294; streamflow analysis, 210–212
- ASCE Standardized Reference ET Equation (ASCE05), 102, 102*e*
- Atlas 14 (NOAA), 29, 29*f*
- atmospheric evaporative demand (E_0): complementarity with ET, 81–83, 82*f*, 129–133; concept of, 71–73; drivers and limits, 74–78, 125–129; evaporation paradox and, 133–134; as limit to ET, 78–79; measurement of, 73–74; models of, 78–101; observations, 96–101; physics of, 73–78; temperature-based formulations, 93–95, 94*f*; trend decomposition, 130–132, 131*f*; trends, 124–129
- autocorrelation: evapotranspiration, 117–120, 118*f*, 119*f*; low flows, 288–299; soil properties, 162–163; streamflow time series, 204, 205*f*
- automated sampling, 400
- autoregressive moving average (ARMA) models: low flow analysis, 290–294; streamflow, 210–212
- Back Creek, West Virginia, flood frequency analysis, 252–255, 253*t*, 254*t*, 255*f*
- basin water balance estimates for ET, 83–85, 83*e*–84*e*, 91
- Baton Rouge, Louisiana, storm duration and depth analysis, 460–461, 462*f*–463*f*, 462*t*, 463–465, 464*t*, 465*f*–466*f*, 467, 468*f*–474*f*, 473, 475*t*–477*t*
- Bayesian methods, 234
- best management practices (BMP) for pollutant removal, 360–374, 361*t*–364*t*, 362*f*–363*f*, 367*f*–370*f*, 371*t*–372*t*, 374*f*
- beta distribution, 388–389
- binomial distribution, 389–390
- bivariate exponential distribution, 414–415, 415*f*
- bivariate extreme value type I distribution, 415–416, 417*f*
- bivariate log-normal distribution, 413–414
- bivariate normal distribution, 412–413, 413*f*
- bootstrap sampling, 46–49, 47*f*, 48*e*, 48*f*
- box-and-whisker plots, 393–394, 393*f*, 396
- Budyko framework for ET, 79–81, 80*e*–81*e*, 80*f*
- Bulletin 13, Methods of Flow Frequency Analysis (IACWR 1966), 235
- Bulletin 15, A Uniform Technique for Determining Flood Flow Frequencies (WRC 1967), 235
- Bulletin 17B, Guidelines for Determining Flood Flow Frequency (IACWD 1982), 234–236, 246–247, 249–252, 257
- Bulletin 17C, Guidelines for Determining Flood Flow Frequency (IACWD), 255–257
- capillary pressure head, 150, 150*f*
- CDFs. *see* cumulative distribution functions
- censored water quality data, 394–396
- channel reaches, 348–351
- Chicago, Illinois, flood control analysis, 354–360, 355*t*, 356*f*–358*f*, 359*t*
- chi-squared test, 193–194, 194*t*, 195*f*

- climate change: flood frequency analysis and, 257–261; low flows and drought and, 325; precipitation frequency analysis and, 51–52
- coefficient of skew: defined, 183, 183e; gamma PDF, 187; log-gamma PDF, 189; log-normal PDF, 185
- coefficient of variation: gamma PDF, 187; log-gamma PDF, 189; log-normal PDF, 185
- complementarity of regional ET and E_0 , 81–83, 82f, 129–133, 131f, 132t
- complex river system modeling, 222–228
- conditional probability adjustment (CPA), 250, 253
- copulas: analytical goodness-of-fit tests, 441–443, 443t–444t, 458–460, 459t–460t, 461f, 467, 473, 475t–477t, 479, 481, 484t; Archimedean, 420–421, 422f, 422t; assessment of fitting, 449, 451, 458–460, 465, 467, 473, 478–479, 481; concept of, 417f, 418; dependence and, 424–436; dependence structure and test space, 446f–448f, 447–448, 461, 463, 463f, 474, 477, 480f; derivation of associated copulas, 424; error statistics of fit, 440–441, 441t, 451, 458, 458t, 467, 475t, 479, 481, 483t; estimation of dependence parameter, 431–436, 448–449, 449t, 464–465, 464t, 477, 480t; exact maximum likelihood method of estimation, 435–436; extreme value, 421, 423; graphical goodness-of-fit methods, 437–438, 438f–441f, 440, 449, 450f–457f, 451, 465, 465f–466f, 467, 468f–474f, 478–479, 481f–483f; invariance property, 424–425; maximum pseudo-likelihood method of estimation, 435; meta-elliptic, 423; miscellaneous, 423–424; moment-like method of estimation, 431, 433–435; nonparametric measures of association, 425–427, 427t; overview, 416–418; peak flow and volume analysis, 444–449, 445f–448f, 449t, 450f–458f, 451, 458–460, 458t–460t, 461f; potential marginal distributions, 445–447, 446f; qualitative assessment of dependence, 427–429, 428f, 430f; random number generation and, 436; regional flood risk analysis, 473–474, 478–479, 478t, 480t, 481–485, 483t–484t; selection process, 436–443, 437f; storm duration and depth analysis, 460–461, 462f–463f, 462t, 463–465, 464t, 465f–466f, 467, 468f–474f, 473, 475t–477t; tail dependence characteristics, 429–431, 432t, 433f–434f; types of, 418–424
- correlation coefficient, 181, 181e
- correlation scale, 181
- CPA (conditional probability adjustment), 250, 253
- crop ET (ET_c). *see* reference crop ET
- cumulative distribution functions (CDFs): copulas, 418, 419f; empirical frequency analysis and, 273–274, 273e, 395; precipitation frequency analysis, 10–11, 11t, 34f
- cumulative probability plots, 10–11, 69f–70f
- daily precipitation time series, 22–23, 22f–23f
- dam effects on low flows, 321–323
- Darcy's Law, 150, 150e
- DARMA modeling: drought length, 302; low flows, 293–294
- decision making aids for infiltration and soil water processes, 172
- derived distribution method, uncertainty analysis, 364
- derived probability distributions: runoff characteristics, 342–354; runoff event peak discharge rate, 343–345; runoff event volume, 343; runoff routing through channel reaches, 348–351; runoff routing through detention ponds, 345–348, 346f; theory, 342–343
- descriptive indexes for precipitation extremes, 53–54, 53t
- deseasonalization, 213–214, 213e–214e
- design storms, 336–337
- detention ponds: flood control analysis, 354–360, 355t, 356f–358f, 359t; runoff routing, 345–348, 346f
- dimensionless relationships in infiltration, 160–162, 161f
- dimming, 126–128
- disaggregation models, 224–228
- discrete ARMA modeling: drought length, 302; low flows, 293–294
- diversion effects on low flows, 321–323
- droughts: climate change and, 325; DARMA modeling, 302; defined, 272, 273f; intensity, 305–307, 320; length, 300–305, 303t, 304f, 305t; magnitude, 305–308, 310–312, 320; overview, 2–3, 269–270; probability distributions, 300–308, 310–316; regional analysis, 319–321; return period,

316–319, 319f; statistical characterization, 299–319

duration: of drought, 272, 273f; of low flow, 271, 271f; of storm, 460–461, 462f–463f, 462t, 463–465, 464t, 465f–466f, 467, 468f–474f, 473, 475t–477t

Durbin-Watson test, 40, 40e

E_0 . *see* atmospheric evaporative demand

eddy covariance technique, 85–88, 85e, 87e

effective saturation, 150, 150e, 150f

El Niño southern oscillation (ENSO), 257–261, 260t, 261t, 262f

EMA. *see* expected moments algorithm

EML (exact maximum likelihood) method, 435–436

empirical analysis: low flows, 273–274; precipitation frequency analysis, 10–11; water quality variables, 395

energy balance modeling, 88–93, 89f, 92f, 93f

ENSO (El Niño southern oscillation), 257–261, 260t, 261t, 262f

enteric bacteria, spring water quality modeling, 198–200, 200f

envelope curves. *see* flood envelope curves

E_{pan} . *see* pan evaporation

EQRM (equi-ratio quantile matching), 36–37, 36f, 37e

ET. *see* evapotranspiration

ET_c (crop ET). *see* reference crop ET

ETCDI (Expert Team on Climate Change Detection and Indexes), 53–54, 53t (ET^{WB}). *see* water balance-derived ET

evaporation. *see* evapotranspiration (ET)

evaporation paradox, 133–134

evapotranspiration (ET): advective limit, 73–74, 73e; atmospheric evaporative demand (*see* atmospheric evaporative demand); autocorrelation, 117–120, 118f, 119f; Budyko framework, 79–81, 80e–81e, 80f; complementarity with E_0 , 81–83, 82f, 129–133; defined, 71; dimming and, 126–128; drivers and limits, 74–78, 125–129, 132–133, 132t; eddy covariance estimation, 85–88, 85e, 86f, 87e; energy and water limits, 79–81; energy balance modeling, 88–93, 89f, 92f, 93f; estimation of, 72; evaporation paradox and, 133–134; GCM modeling and, 122; global observations, 121–122; Mann-Kendall test, 117–120, 119f; measurement of, 73–74;

models, 78–101; moisture availability limit, 74–75, 74e; overview, 2; Penman-Monteith approach, 101–102, 102e; physics of, 73–78; radiative driver, 76–78, 76e–77e, 76f; reference crop ET (*see* reference crop ET); regional trends across CONUS, 123–125, 123f; remote sensing and, 88–93, 89f, 92f, 93f; stilling and, 128–129; trend analysis, 116–134; utilization of concept, 71–72; water balance estimates, 83–85, 83e–84e, 91

exact maximum likelihood (EML) method, 435–436

exceedance probability of envelope curves, 516–522, 519f, 521f, 522t

expected moments algorithm (EMA), 252, 253–255, 254t, 255f, 256–257, 263–264

expected value: gamma PDF, 186; log-gamma PDF, 188; log-normal PDF, 184

Expert Team on Climate Change Detection and Indexes (ETCDI), 53–54

exponential distribution: bivariate, 414–415, 415f; groundwater hydrology, 186; hydraulic conductivity data, 195–196, 196t; precipitation data, 13; record events, 495t, 500

extreme events: droughts (*see* droughts); floods (*see* flood frequency analysis); precipitation (*see* precipitation extremes); record events (*see* record events)

extreme value copulas, 421, 423

extreme value type I distribution: hydrologic analysis, 415–416, 417f; precipitation extremes, 12; record events, 495t, 496–498, 497f

extreme value type III distribution: low flow frequency analysis, 279–280, 280f; precipitation data, 12; water quality variables, 388–389

FARMA (fractionally differenced autoregressive moving average) models, 218–220

FDCs (flow duration curves), 321–322, 324f

first-order gamma-autoregressive modeling, 291–295, 295f, 295t

first-order second moment, uncertainty analysis, 364–365

flood control. *see* urban stormwater management

flood envelope curves: basic formula, 509, 509e; empirical, 519–522, 521f, 522t; exceedance probability, 516–522, 519f, 521f, 522t;

- historical background, 508*f*, 509, 510*t*, 511;
overview, 508–509; probabilistic
interpretation of, 513–519, 514*f*, 522–526,
523*f*, 524*t*, 525*f*, 526*t*, 527*f*–528*f*;
relationships, 511–512, 512*f*, 513*f*; theory of
records and, 515–516, 515*f*; traditional
applications, 509, 511
- flood frequency analysis: annual flood series
model, 240–243; block adjustment, 257–258;
case studies of record events, 522–532;
copula-based analysis, 473–474, 478–479,
478*t*, 480*t*, 481–485, 483*t*–484*t*; envelope
curves (*see* flood envelope curves); estimation
procedures, 245–257; expected moments
algorithm, 252, 253–255, 254*t*, 255*f*, 256–257,
263–264; historical information and, 250–252,
251*f*, 256–257, 262; log-Pearson type III
distribution and, 234, 236–238, 240–244; low
outliers, 249–250, 252–253, 256, 262; method
of moments (MOM), 245–248; moments of
number of record events, 503–504, 505*t*;
multivariate distributions, 410–412, 504–508,
506*t*; nonparametric properties of record
events, 501–508; overview, 2, 233–234;
parametric adjustment, 257–258; parametric
properties of record events, 494–501;
parametric relationships, 258–259; probability
distribution of number of record events, 503,
504*f*; recommendations under development,
255–257; record theory and, 491–533;
recurrence time for record event, 501–502,
502*e*; regional risk analysis, 473–474, 478–479,
478*t*, 480*t*, 481–485, 483*t*–484*t*; runoff routing
through channel reaches, 348–351; theory of
records and, 526–531, 529*f*–531*f*, 531*t*; waiting
time for record event, 501–502, 502*e*
- Florida: annual precipitation extreme, example,
24*t*–25*t*, 24–26, 26*f*; climate cycles and
rainfall, 51–52, 52*f*; intensity-duration-
frequency curve for rainfall, 26–28, 27*f*
flow duration curves (FDCs), 321–322, 324*f*
FLUXNET, 85, 86*f*
- fractional Gaussian noise model, 217–218
- fractionally differenced autoregressive moving
average (FARMA) models, 218–220
- frequency analysis: of floods (*see* flood
frequency analysis); of low flows, 273–274
- frequency distributions, 28–29, 29*f*
- frequency factors, 18–19
- gamma distribution: drought magnitude, 307,
309*t*–310*t*; groundwater hydrology, 185–188;
precipitation data, 13; residence time and age
of groundwater, 196–198, 197*f*; spring water
quality modeling, 198–200, 200*f*; water
quality variables, 388–389
- Gauley subbasin, West Virginia, regional flood
risk analysis, 473–474, 478–479, 478*t*, 480*t*,
481–485, 483*t*–484*t*
- Gaussian distribution. *see* normal distribution
- general circulation model (GCM) simulations:
evapotranspiration and, 122; precipitation
extremes and, 56
- generalized extreme value (GEV) distribution:
low flow series, 280–282, 281*f*; precipitation
data, 13; record events, 495*t*, 498–500, 499*f*
- generalized Pareto distribution, 495*t*, 500–501
- geometric mean, 182, 182*e*
- geostatistical scaling methods, 162–163, 163*f*,
164*f*
- Geum River basin, Korea, low flow analysis,
322, 323*f*
- GEV distribution. *see* generalized extreme value
distribution
- glossaries: record events, 491–492; water quality
variables, 381–383
- goodness-of-fit tests: annual extremes for
different durations, 24*t*–25*t*, 24–26, 26*f*;
copula selection, 437–438, 438*f*–441*f*,
440–443, 443*t*–444*t*, 449, 450*f*–457*f*, 451,
458–460, 459*t*–460*t*, 461*f*, 465, 465*f*–466*f*,
467, 468*f*–474*f*, 473, 475*t*–477*t*, 478–479, 481,
481*f*–483*f*, 484*t*; daily precipitation time
series, 22–23, 22*f*–23*f*; hydraulic conductivity
data, 193–194, 194*t*, 195*f*; L-moment
diagrams, 21; normal distributions, 20;
quantitative measures, 21
- gravity drainage, 152
- Greenbrier River, West Virginia, peak flow and
volume analysis, 444–449, 445*f*–448*f*, 449*t*,
450*f*–458*f*, 451, 458–460, 458*t*–460*t*, 461*f*
- Greenbrier subbasin, West Virginia, regional
flood risk analysis, 473–474, 478–479, 478*t*,
480*t*, 481–485, 483*t*–484*t*
- green building design principles, 352–354
- ground-based measurements of precipitation,
6–7
- groundwater hydrology: coefficient of skew,
183, 183*e*; geometric mean, 182, 182*e*;

- notations for aquifer properties, 182;
- overview, 2; probability density functions, 183–190; probability distributions, 179–201; residence time and age, 196–198, 197f; sample average, 182, 182e; spring water quality modeling, 198–200, 200f; standard deviation, 182–183, 182e–183e; statistical definitions, 180–181; variance, 182
- Guidelines for Determining Flood Flow Frequency, Bulletin 17 series (IACWD), 234–236, 246–247, 249–252, 255–257
- Gumbel distribution. *see* extreme value type I distribution
- Han River basin, Korea, low flows analysis, 322, 323f–325f
- historical information: flood frequency analysis and, 250–252, 251f, 256–257, 262; precipitation frequency analysis and, 31–32
- homogeneity: E_{pan} data, 99–101; precipitation extremes, 42–44; statistical, 181
- homogeneous region selection for low flow analysis, 284–285
- Hortonian overland flow, 151
- Hurst effect, 162, 207–208, 217–221
- hydraulic conductivity: aquifers, 179, 180f; exponential PDF application, 195–196, 196t; infiltration and, 150–151; log-gamma PDF application, 192–194, 193f, 194t, 195f; log-normal PDF application, 191–192, 191f–192f; temporal variability, 158–160; vertical soil heterogeneity, 156
- HYDRO-35, 28–29
- hydrologic analysis: bivariate exponential distribution, 414–415, 415f; bivariate extreme value type I distribution, 415–416, 417f; bivariate log-normal distribution, 413–414; bivariate normal distribution, 412–413, 413f; copula method, 416–443 (*see also* copulas); flood events, 410–412; hydrometeorological applications, 408–410; multivariate distributions, 408–416; overview, 3, 407–408
- hydrologic cycle: evapotranspiration (*see* evapotranspiration); floods (*see* flood frequency analysis); groundwater (*see* groundwater hydrology); infiltration (*see* infiltration); multivariate frequency distributions in (*see* hydrologic analysis); precipitation extremes (*see* precipitation extremes); record events (*see* record events); soil water (*see* soil water); stormwater management and (*see* urban stormwater management); streamflow (*see* streamflow)
- hydrologic design: future data sources, 52–53; future of, 57
- hypergeometric distribution, 390
- IDF (intensity-duration-frequency) curves: precipitation extremes, 26–28, 27f
- IDWM (inverse distance weighting method), 32–33
- IETD (interevent time definition), 51
- IHA (Indicator of Hydrologic Alteration), 321–322, 322t
- impervious areas, 340, 341
- independence: defined, 181; evaluation of, 49–50
- Indicator of Hydrologic Alteration (IHA), 321–322, 322t
- infilling methods, 34–35, 34f
- infiltrability. *see* infiltration capacity (f_c)
- infiltration: acronyms and symbols, 172–173; approximation techniques, 153; boundary and initial conditions, 152; capillary pressure head, 150, 150f; cumulative, 151; decision support systems, 172; dimensionless relationships, 160–162, 161f; dynamics of, 151–153; effective parameters of heterogeneous soil, 163–165; effective saturation, 150, 150e, 150f; engineering treatment of, 148; geostatistical scaling, 162–163, 163f, 164f; Hortonian overland flow, 151; hydraulic conductivity and, 150–151; hydrologic process interactions, 145–147, 146f, 148f; local measurement uncertainty, 166–167; local processes, 150–151; numerical solution methods, 152–153; overview, 2; parameter estimation, 167; pedotransfer functions and, 160, 161f; plant canopy and, 148–149, 149f; quantification challenges, 170–171; Richard's Equation, 151, 151e; runoff and, 168–170; scaling and estimation, 160–165; soil-surface sealing and, 153–154; soil-water content measurement, 154, 155f; sorptivity, 156; space-time simulations, 168–172; spatial variability, 156–158, 158f, 159f, 159t; surface flux measurements, 154–156; temporal variability, 158–160; uncertainty, 147, 166–168; variability, 147, 156–160; vertical soil heterogeneity and, 156;

- water transfer process, 150–151; wetting process, 150–151
- infiltration capacity (f_c), 146–147, 151, 160–162, 161*f*
- intensity-duration-frequency (IDF) curves, 26–28, 27*f*
- interevent time definition (IETD), 51, 338
- intermittent flows, 216–217, 282–283, 283*f*
- interpolation methods, 32–37, 34*f*
- invariance property of copulas, 424–425
- inverse distance weighting method (IDWM), 32–33
- inverse methods, 167
- joint probability distributions: drought characteristics, 312–316; regional flood risk analysis, 481–485, 484*f*–485*f*
- Kaplan Meier approach, 395
- k-C* model, 360–371, 361*t*–364*t*, 362*f*–363*f*, 367*f*–370*f*
- kernal density estimation (KDE), 46, 46*e*
- k-nearest neighbors resampling (KNNR), 221–222
- LAI (leaf area index), 148–149
- land surface temperature, 93–95, 94*f*
- Las Palmas Creek, California, spring water quality, 198–200, 200*f*
- Latin hypercube sampling, uncertainty analysis, 365
- leaf area index (LAI), 148–149
- LFCs (load frequency curves), 372–373, 374*f*
- linear regression, 39–42
- Little River, North Carolina, flood frequency analysis, 247–248, 248*t*, 249*f*
- Ljung-Box Q test, 40–42, 41*e*
- L-moment analysis: flood frequency analysis, 243–244, 244*f*, 244*t*; precipitation data, 17–18, 21
- load frequency curves (LFCs), 372–373, 374*f*
- log-gamma distribution. *see* log-Pearson type III distribution
- log-normal distribution: bivariate, 413–414; groundwater hydrology, 183–185; hydraulic conductivity data, 191–192, 191*f*–192*f*; low flow series, 276–278, 278*f*, 278*t*; precipitation data, 12, 12*e*; water quality variables, 387–388
- log-Pearson type III distribution: annual flood series model, 240–243, 242*f*; characteristics of, 236–244; defined, 13, 237–238, 237*e*, 239*f*, 240*t*; flood frequency analysis and, 234, 255–256; groundwater hydrology, 188–190; hydraulic conductivity data, 192–194, 193*f*, 194*t*, 195*f*; L-moments, 243–244, 244*f*, 244*t*; log space characteristics, 236, 240–241; low flow series, 274–276, 276*t*; real space characteristics, 237–238, 241–242
- log space method of moments, 245–248
- long memory models, 218–220
- Los Angeles, California, BMP performance for pollutant removal, 371–374, 371*t*–372*t*, 374*f*
- low flows: ARMA modeling, 290–294; autocorrelated flow analysis, 288–299; climate change and, 325; DARMA modeling, 293–294; defined, 270–272, 271*f*; empirical frequency analysis, 273–274; extreme value type III distribution, 279–280, 280*f*; first-order gamma-autoregressive modeling, 291–295, 294*t*, 295*f*; fitting of univariate distributions, 274–282; generalized extreme value distribution, 280–282, 281*f*; hydraulic structures and, 321–323, 322*t*, 323*f*–325*f*; intermittent flows, 282–283, 283*f*; log-Pearson type III distribution, 274–276, 276*t*; overview, 2–3, 269–270; probability distribution, 274–283; regional analysis, 283–288 (*see also* regional analysis of low flows); return period and risk, 295–299, 298*f*, 298*t*–299*t*; simple Markov chain modeling, 288–290, 289*f*; three-parameter log-normal distribution, 276–278, 278*f*, 278*t*
- low-impact development practices, 352–354
- LP3 distribution. *see* log-Pearson type III distribution
- MADI (mean absolute deviation index), 21
- Mann-Kendall test: evapotranspiration, 117–120, 119*f*; precipitation extremes, 38–39, 38*e*–39*e*, 41*f*
- Mann-Whitney U statistic, 43, 43*e*
- Mapocho River, Chile, low flow analysis, 294–295, 294*t*, 295*f*
- maximum likelihood estimation method, 17
- maximum pseudo-likelihood (MPL) method, 435
- mean absolute deviation index (MADI), 21
- mean square deviation index (MSDI), 21
- measurements: censored water quality data, 394–396; evapotranspiration, 73–74;

- infiltration, 166–168, 171; precipitation, 6–9; soil-water content, 154, 155*f*, 166–168, 171; statistical homogeneity and independence, 181; surface flux, 154–156
- median: gamma PDF, 186; log-gamma PDF, 189; log-normal PDF, 184
- meta-elliptic copulas, 423
- method of moments (MOM): copula dependence parameters, 431–435, 448–449, 449*t*, 464–465, 464*t*; flood frequency analysis, 245–248; precipitation extremes, 16–17; reference crop ET, 106–115, 108*f*–114*f*; with regional skew, 246–248
- Methods of Flow Frequency Analysis, Bulletin 13 (IACWR 1966), 235
- MGBT (multiple Grubbs-Beck outlier test), 256–257
- mode: gamma PDF, 187; log-gamma PDF, 189; log-normal PDF, 184
- model process uncertainty, 167
- moisture availability limit for ET, 74–75, 74*e*
- moments: detection of changes, 44–45, 45*t*; of distributions, 19*t*; drought length, 300–305; estimation of distribution parameters, 17–18; expected moments algorithm, 252, 253–255, 254*t*, 255*f*, 256–257, 263–264; first-order second moment, uncertainty analysis, 364–365; gamma PDF, 187; L-moments approach (*see* L-moment analysis); log-gamma PDF, 189–190; method of moments, 16–17; number of record events, 503–504, 505*t*; record event analysis, 496
- MPL (maximum pseudo-likelihood) method, 435
- MSDI (mean square deviation index), 21
- multinomial distribution, 391
- multiple Grubbs-Beck outlier test (MGBT), 256–257
- multivariate analysis: hydrological variables, 407–485 (*see also* hydrologic analysis); record events, 504–508, 506*t*; time series modeling, 223–224; water quality variables, 401–402
- negative binomial distribution, 391
- New River, Virginia, flood risk forecast, 259–261, 260*t*, 261*t*, 262*f*
- NEXt Generation RADar (NEXRAD), 7–8, 8*f*
- Niger River, 220, 220*e*
- NLDAS (North American Land Data Assimilation System), 106–108
- nonparametric methods: bootstrap sampling, 46–49, 47*f*, 48*e*, 48*f*; copulas and, 425–427, 427*t*; estimation of quantiles and proportions, 391–393; independence evaluation, 49–50; kernel density estimation, 46, 46*e*; precipitation extremes, 45–50; ranked von Neumann test, 50, 50*e*; record event analysis, 501–508; runs test, 48–50, 49*e*–50*e*; streamflow modeling, 221–222; water quality variables, 391–394
- normal distribution: bivariate, 412–413, 413*f*; goodness-of-fit tests, 20; precipitation data, 12, 12*e*; water quality variables, 358–386
- normality testing of water quality, 386–387
- North American Land Data Assimilation System (NLDAS), 106–108
- North Central Italy, probabilistic regional envelope curves, 523–524, 523*f*, 524*t*
- outliers in flood frequency analysis, 249–250, 252–253, 256, 262
- pan evaporation (E_{pan}). *see* E_{pan} : decomposition of trends, 129–130; derivation of E_0 , 94–96; evaporation paradox and, 133–134; observed E_0 , 96–97; trend analysis and, 116, 124–125; uncertainty and limitations, 97–101
- Paraná River, Argentina, low flow return period and risk, 297–299, 298*f*, 298*t*–299*t*
- PARMA streamflow models, 214–216
- partial duration series, 50–51
- PDFs. *see* probability density functions
- Pearson type III distribution: defined, 236, 236*e*, 237*f*; precipitation data, 13
- pedotransfer functions (PTFs), 160, 161*f*
- Penman-Monteith approach to ET, 101–102, 102*e*
- Penns Creek, Pennsylvania, low flow estimation, 275–276, 276*t*
- performance modeling for BMP pollutant removal: description of k-C* model, 360–364; k-C* model, 361*t*–364*t*, 362*f*–363*f*; load frequency curve approach, 372–373, 374*f*; overview, 360; sensitivity, 365–371, 367*f*–370*f*; uncertainty, 361–363, 365–374
- periodic autoregressive moving average (PARMA) models, 214–216
- periodicity of streamflows, 206, 206*f*
- pervious areas, 341

- Philip's infiltration equation, 153, 153e, 157, 158t
- physics of evapotranspiration, 73–78
- PILFs (potentially influential low floods), 256
- plant canopy interception of rainfall, 148–149, 149f
- PMP (probable maximum precipitation), 30–31
- Poisson distribution, 338–339, 390–391
- ponding time, 151, 152, 152f
- population of interest, defining, 396–397
- porosity of common rocks, 179, 180t
- potentially influential low floods (PILFs), 256
- Poudre River, Colorado: drought intensity analysis, 306–307; drought length analysis, 302–305, 303t, 304f, 305t; drought magnitude analysis, 306–307; drought return period analysis, 317–319, 319f; streamflow variability analysis, 208–209, 208f–209f
- precipitation extremes: annual extremes for different durations, 24t–25t, 24–26, 26f, 50–51, 69f–70f; bootstrap sampling, 46–49, 47f, 48e, 48f; changes in moments, 44–45, 45t; characterization of data, 11–13, 14t–16t; copula-based analysis, 460–461, 462f–463f, 462t, 463–465, 464t, 465f–466f, 467, 468f–474f, 473, 475t–477t; cumulative distribution functions, 10–11; daily precipitation time series, 24, 24f, 25f; descriptive indexes, 53–54, 53t; distribution parameter estimation, 19–20; droughts (*see* droughts); E_{pan} errors, 98–99; errors in measurement, 6; estimation, 7–9; frequency factors, 18–19; GCM simulations, 56; goodness-of-fit tests, 20–26; ground-based measurement, 6–7; homogeneity, 42–44; independence evaluation, 49–50; interevent time definition, 51; kernel density estimation, 46, 46e; linear regression, 39–42; Mann-Kendall test, 38–39, 38e–39e, 41f; Mann-Whitney U statistic, 43, 43e; measurement, 5–9; monitoring networks, 6–7; nonparametric methods, 45–50; overview, 1, 5; parametric frequency curves, 26–28, 27f; partial duration series, 50–51; precipitation frequency analysis (*see* precipitation frequency analysis); probability distributions, 9–13; probable maximum precipitation, 30–31; quantile mapping, 35–37, 36f, 37e; radar-based measurements, 7–9, 52–53; ranked von Nuemann test, 50; as record events, 492; regional envelope curves, 525–526, 525f, 526t, 527f–528f; regional frequency analysis, 21–22; runs test, 48–50, 49e–50e; satellite-based measurement, 9; Spearman's rank correlation coefficient (ρ) test, 37–38, 37e, 39, 40f; standard precipitation index, 54–56, 54e–55e; stationarity issues, 37–42; storm duration and depth analysis, 460–461, 462f–463f, 462t, 463–465, 464t, 465f–466f, 467, 468f–474f, 473, 475t–477t
- precipitation frequency analysis: annual extreme value series, 50–51; climate change and, 51–52; cumulative distribution functions, 10–11, 11t; estimation in, 32–35; future data sources, 52–53; GCM simulations, 56; length of historical data, 31–32; missing data, 32–36, 34f, 36f; regional, 21–22; sample adjustment factors, 31; uncertainty and variability, 31–37; for United States, 28–29, 29f
- preferential flow, 167
- principal component analysis, 401–402
- probability density functions (PDFs). *see also specific probability distributions*: defined, 180–181; groundwater hydrology, 183–190; maximum likelihood estimation method, 17; precipitation data, 11–13; standard precipitation index, 54–56, 54e–55e
- probability distributions. *see also specific probability distributions*: annual precipitation extreme, example, 24t–25t; characterization of precipitation data, 11–13, 14t–16t; derived, 342–354; drought characteristics, 300–316; drought intensity, 305–307; drought length, 300–305; drought magnitude, 305–308, 309t–310t, 310–312; evaluation of residuals, 41t; flood frequency analysis, 233–234; frequency factors, 18–19; goodness-of-fit tests, 20–26; in groundwater hydrology, 179–201; moments, 17–18, 19t, 21; number of record events, 503, 504f; overview, 11; parameter estimation, 16–18; precipitation extremes, 9–10, 13; record theory and, 493–494; stormwater modeling, 336–338; water quality variables, 384–403
- probability sampling: serial correlation and, 399; water quality variables, 397
- probability-weighted moments (PWM), 17–18
- probable maximum precipitation (PMP), 30–31

proportions, nonparametric estimation, 392–393
ProUCL, 387
PTFs (pedotransfer functions), 160, 161f
PWM (probability-weighted moments), 17–18

quantile mapping, 35–37, 36f, 37e
quantiles: censored data, 396; log-gamma PDF, 190; log-normal PDF, 185, 187–188; nonparametric estimation, 391–393; record event analysis, 496

radar-based measurements of precipitation, 7–9, 8f
radiative driver for ET, 76–78, 76f, 126–128
rainfall: characterization of local conditions, 338–340; conversion from exceedance probability to return period, 351–352; droughts (*see* droughts); extremes (*see* precipitation extremes); frequency analysis (*see* precipitation frequency analysis); infiltration (*see* infiltration); multivariate distributions, 408–410; probabilistic models, 339–340, 339t; runoff generation, 340–341; separation of events, 338–339; water harvesting storage unit sizing, 352–354
rain gauges, 6–7
random number generation, 436
ranked von Neumann test, 50, 50e
record events: case studies, 522–532; definitions, 491–492; exponential distribution, 495t, 500; extreme value type I distribution, 495t, 496–498, 497f; flood envelope curves (*see* flood envelope curves); generalized extreme value distribution, 495t, 498–500, 499f; generalized Pareto distribution, 495t, 500–501; moments of number of events, 503–504, 505t; multivariate distributions, 504–508, 506t; nonparametric properties, 501–508; overview, 3; parametric properties, 494–501; probability distribution of number of events, 503, 504f; properties of United States floods, 526–531, 529f–531f, 531t; recurrence time, 501–502, 502e; theory of, 492–494; waiting time, 501–502, 502e
recurrence time for record event, 501–502, 502e
reference crop ET (ET_{rc}): approach, 79; ASCE05, 102, 102e; concept of, 71–72, 101; derivation of crop ET from reference ET,

102–103; method of moments variability analysis, 106–115, 108f–114f; Penman-Monteith approach to ET, 101–102, 102e; sensitivity analysis, 104–106, 105f; uncertainty, 103–104
regional analysis of droughts, 319–321
regional analysis of low flows: baseflow correlation, 286–288; homogeneous region selection, 284–285; overview, 283; regression model, 285–286
regional envelope curves, 513–519, 514f, 522–526, 523f, 524t, 525f, 526t, 527f–528f
regional frequency analysis of precipitation extremes, 21–22
regression models, 285–286
regression on order statistics (ROS), 395
remote sensing: energy balance modeling of ET and, 88–93, 89f, 92f, 93f; soil-water content, 171
reservoirs, 207–209
residence time and age of groundwater, 196–198, 197f
return period: droughts, 316–319, 319f; low flows, 295–299, 298f, 298t–299t; urban stormwater management, 351–352
Richard's Equation, 151, 151e
risk assessment: infiltration and soil water processes, 172; low flows, 295–299, 298f, 298t–299t; regional flood risk analysis, 473–474, 478–479, 478t, 480t, 481–485, 483t–484t
rivers: flood frequency (*see* flood frequency analysis); low flows (*see* low flows); record events (*see* record events); streamflow modeling (*see* streamflow); water quality (*see* water quality)
ROS (regression on order statistics), 395
runoff: derived probability distributions, 342–354; detention ponds and, 345–348; infiltration and, 168–170; overview, 3; peak discharge rate, 343–345; rainfall transformation, 340–341; routing through channel reaches, 348–351; saturation excess overland flow, 151; volume, 343
run-on, 168
runs test, 48–50, 49e–50e

Salso River, Italy, drought magnitude analysis, 308, 310t, 311–312, 312t, 316–317
sample adjustment factors, 31

- sample average, 182, 182*e*. *see also* expected value
- San Pedro River, Mexico, low flow estimation, 277–282, 278*f*, 278*t*, 280*f*, 281*f*
- satellite-based measurements of precipitation, 9
- saturated hydraulic conductivity, 150–151, 164–165, 165*f*, 168–170, 169*f*, 170*f*
- scaling, 160–165, 168–170
- seasonality: evapotranspiration, 125;
streamflow modeling, 213–216; streamflow time series, 204–206; water quality, 400–401
- SEEB (Simplified Surface Energy Balance)
modeling, 89*f*, 92*f*–93*f*
- sensitivity analysis: performance modeling of
pollutant removal, 365–371, 367*f*–370*f*;
reference crop ET, 104–106, 105*f*
- serial correlation: automated sampling and, 400;
nearly continuous monitoring and, 400;
probability sampling and, 399; stochastic processes, 399; trend analysis and, 399–400;
water quality, 398–400
- shifting mean models, 220–221
- simple Markov chain, 288–290, 289*f*
- Simplified Surface Energy Balance (SSEB)
modeling, 88–93, 89*f*, 92*f*–93*f*
- snowfall. *see* precipitation extremes
- software: infiltration and soil water processes, 172; streamflow modeling, 228; water quality data, 387, 389
- soil properties: effective parameters of
heterogeneous soil, 163–165; infiltration and, 148; pedotransfer functions and, 160, 161*f*;
scaling of, 160–165; soil-surface sealing, 153–154; surface flux measurements, 154–156; temporal variability, 158–160; water content measurement, 154, 155*f*
- soil water. *see also* infiltration: acronyms and symbols, 172–173; hydrologic process interactions, 145–147, 146*f*, 147*f*; local processes, 150–151; measurement methods, 154, 155*f*, 166–168, 171; space-time simulations, 168–172; spatial variability, 156–158, 158*f*, 158*t*, 159*f*, 159*t*; temporal variability, 158–160; uncertainty, 147, 166–168; variability, 147, 156–160
- sorptivity, 156
- spatial correlation, 181
- spatial interpolation methods, 32–37, 36*f*
- spatial variability of infiltration, 156–158, 158*f*, 158*t*, 159*f*, 159*t*
- Spearman's rank correlation coefficient (ρ) test, 37–38, 37*e*, 39, 40*f*
- spring water quality modeling, 198–200, 200*f*
- SSEB (Simplified Surface Energy Balance)
modeling, 88–93
- standard deviation, 182–183, 182*e*–183*e*
- standard precipitation index, 54–56, 54*e*–55*e*
- stationarity, 37
- statistical analysis. *see also specific statistical methods*: droughts, 299–319;
evapotranspiration, 71–135; precipitation extremes, 5–57
- statistical homogeneity, 181
- statistical inference: aquifer properties, 182–183; infiltration and soil water, 167–168
- stilling, 128–129
- stochastic modeling: serial correlation and, 399;
streamflow variability, 203–229; water quality data, 397–398
- storm events. *see* precipitation extremes
- stormwater management. *see* urban stormwater management
- streamflow: ARMA models, 210–212;
autocorrelation, 204; complex river system modeling, 222–228; copula-based analysis, 444–449, 445*f*–448*f*, 449*t*, 450*f*–458*f*, 451, 458–460, 458*t*–460*t*, 461*f*; defined, 203;
deseasonalization, 213–214, 213*e*–214*e*;
disaggregation models, 224–228; flow regime, 321–322; fractional Gaussian noise model, 217–218; Hurst effect, 207–208; intermittent flow models, 216–217; long memory models, 218–220; long-term variability models, 217–221; low flows (*see* low flows); modeling strategies for complex river systems, 226–228; multivariate time series modeling, 223–224; nonparametric modeling, 221–222; overview, 2; peak flow and volume analysis, 444–449, 445*f*–448*f*, 449*t*, 450*f*–458*f*, 451, 458–460, 458*t*–460*t*, 461*f*; periodic models, 214–216; product models for intermittent flows, 216–217; seasonality, 204–206; seasonal series modeling, 213–216; shifting mean models, 220–221; software tools, 228; stochastic features, 203–209; stochastic modeling, 209–222; storage-related statistics, 207–209; variability modeling, 203–229; water quality and, 400–401
- surface energy balance modeling of ET, 88–93, 89*f*, 92*f*, 93*f*

- surface flux measurements, 154–156
- surface infiltration. *see* infiltration
- surface seal, 153–154
- symbols: infiltration and soil water, 172–173; urban stormwater management, 333–335
- Technical Paper (TP) 40, 28–29
- temperature-based formulations of E_0 , 93–95, 94f
- temporal variability of soil properties, 158–160
- tension infiltrometer methods, 155
- three-parameter log-normal distribution: low flow series, 276–278, 278f, 278t; precipitation data, 12
- time series for streamflow: autocorrelation, 204, 205f; Hurst effect, 207–208; modeling, 209–222; seasonality, 204–206; stochastic features, 203–209; storage-related statistics, 207–209
- time series for water quality, 397–398
- TP-40, 28–29
- transformations of water quality data, 386–387
- trend analysis: evapotranspiration, 116–134; precipitation extremes, 37–42, 42f; serial correlation and, 399–400
- Tropical Rainfall Measuring Mission (TRMM), 9
- t-tests, 44–45
- Twelve Mile Creek, North Carolina, low flow estimation, 283, 283f
- Tyrol, Austria, probabilistic regional envelope curves, 525–526, 525f, 526t, 527f–528f
- uncertainty. *see also* variability: analysis methods, 364–365; derived distribution method, 364; evapotranspiration, 72; first-order second moment, 364–365; infiltration and soil water, 147, 166–168; k-C* model and, 361–363; Latin hypercube sampling, 365; pollutant removal BMP performance modeling, 361–363, 365–374; precipitation frequency analysis, 31–37; reference crop ET (ET_{rc}), 103–104; sensitivity, 365–370, 367f–370f
- Uniform Technique for Determining Flood Flow Frequencies, Bulletin 15 (WRC 1967), 235
- United States: flood frequency analysis, 233–264 (*see also* flood frequency analysis); precipitation frequency analysis, 28–29, 29f; record-breaking floods, 526–531, 529f–531f, 531t
- universal multifractal models, 168–170, 169f, 170f
- Upper Colorado River basin, disaggregation models, 227–228
- urban stormwater management: analytical probabilistic models, 336–360; conversion from exceedance probability to return period, 351–352; derived probability distributions for runoff characteristics, 342–354; flood control analysis, 354–360, 355t, 356f–358f, 359t; overview, 3; pollutant removal performance modeling, 360–374, 361t–364t, 362f–363f, 367f–370f, 371t, 372f; rainfall characterization, 338–340; rainfall-runoff transformation, 340–341; runoff event peak discharge rate, 343–345; runoff event volume, 343; runoff routing through channel reaches, 348–351; runoff routing through detention ponds, 345–348, 346f; symbols, 333–335
- variability. *see also* uncertainty: infiltration and soil water, 147; precipitation frequency analysis, 31–37; reference crop ET, 106–115, 108f–114f
- variance: defined, 182; gamma PDF, 187; log-gamma PDF, 189; log-normal PDF, 185
- von Neumann's ratio test, 50, 50e
- waiting time for record event, 501–502, 502e
- Wald-Wolfowitz test, 48–50, 49e–50e
- water balance-derived ET (ET^{WB}), 83–85, 83e–84e, 91, 132–134, 132t
- water management. *see* urban stormwater management
- water pollution: BMP performance modeling, 360–374, 361t–364t, 362f–363f, 367f–370f, 371t–372t, 374f; microbiological contaminants, 390–391
- water quality: analysis of variables, 381–403; beta distribution, 388–389; binomial distribution, 389–390; box-and-whisker plots, 393–394, 393f; censored observations, 394–396; definitions, 381–383; extreme value type III distribution, 388–389; gamma distribution, 388–389; hypergeometric distribution, 390; log-normal distribution, 387–388; microbiological variables, 390–391; multinomial distribution, 391; multivariate

- characterization, 401–402; negative binomial distribution, 391; nonparametric representations of data, 391–394; normal distribution, 358–386; normality testing of data, 386–387; overview, 3, 383; Poisson distribution, 390; population of interest, defining, 396–397; practical applications of distributions, 384–385; probability sampling, 397; seasonality, 400–401; serial correlation, 398–400; special characteristics of variables, 383–384; springs, 198–200, 200*f*; stochastic processes, 397–398; streamflow and, 400–401; time series, 397–398; transformation of data, 386–387
- Water Resources Council (WRC), 235
- Water Resources Planning Act, 235
- water table, infiltration and, 152
- Watson, Keith, 157
- Weather Surveillance Radar 88-Doppler (WSR 88-D), 7–8, 8*f*
- Weibull distribution. *see* extreme value type III distribution
- WRC (Water Resources Council), 235
- WSR 88-D (Weather Surveillance Radar 88-Doppler), 7–8, 8*f*
- Z-statistic. *see* Mann-Kendall test